

# Polarization Engineering *through* Nanoengineered Morphology

*Akhlesh Lakhtakia*

Department of Engineering Science and Mechanics

*The Pennsylvania State University*

**March 27, 2007**

Electromagnetics, Remote Sensing, and Space Sciences

Seminar

**Department of Electrical Engineering**

**Penn State**

# Optics Practice

## Control of

- Intensity
- Operating frequency band
- Polarization state

# Optics Practice

## Long History

- Intensity
- Operating frequency band

## Short History

- Polarization state

# Optics Practice

## Polarization

– Discovered in 1809



Etienne-Louis Malus  
1775 - 1812

# Optics Practice

## Polarization

- Discovered in 1809



Etienne-Louis Malus  
1775 - 1812

- “Do not disturb” designs

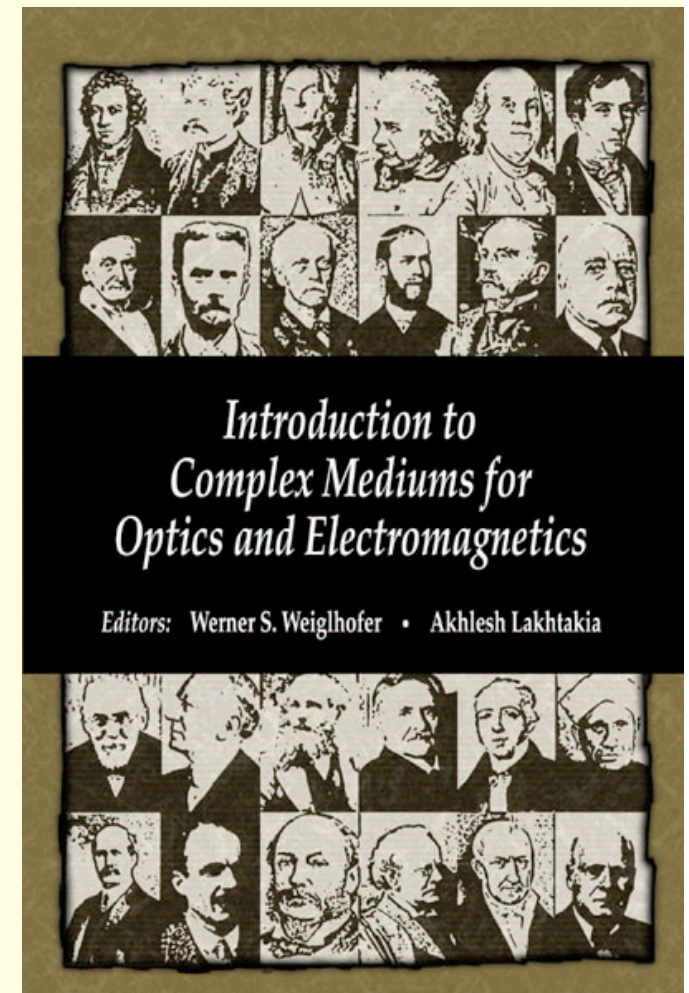
# Polarization Engineering

- Anisotropic materials
  - *Uniaxial and biaxial crystals*
  - *Piezoelectric materials*
  
- Bianisotropic materials
  - *Chiral materials*
  - *Magnetolectric materials*

# Polarization Engineering

- Anisotropic materials
- Bianisotropic materials

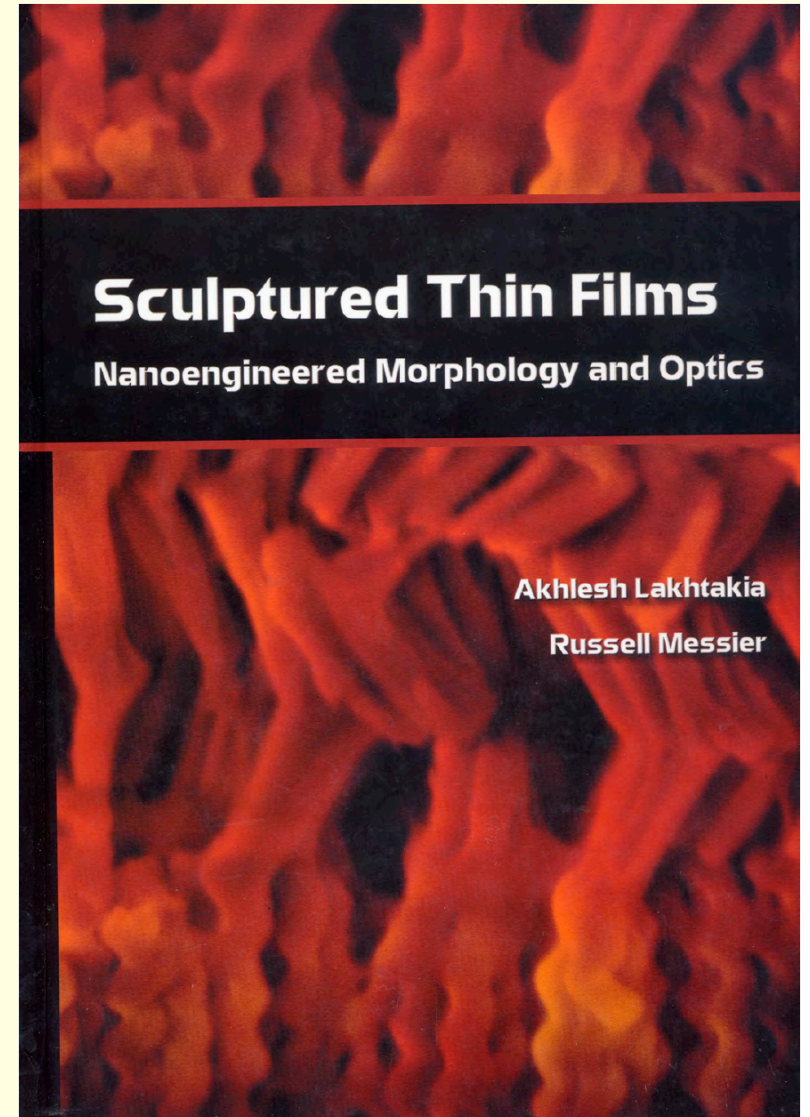
SPIE Press (2003)



# Polarization Engineering

– Sculptured Thin Films

SPIE Press (2005)





# Students & Collaborators

- Joseph Sherwin, Sean Pursel, Benjamin Ross, Fei Wang (Penn State)
- Mark Horn, Jian Xu (Penn State)
- Ian Hodgkinson (Otago)
- Martin McCall (Imperial)
- John Polo (Edinboro)

# Outline

- Introduction
- Optical Modeling
- Examples of Polarization Engineering
- More Examples
- What's next?

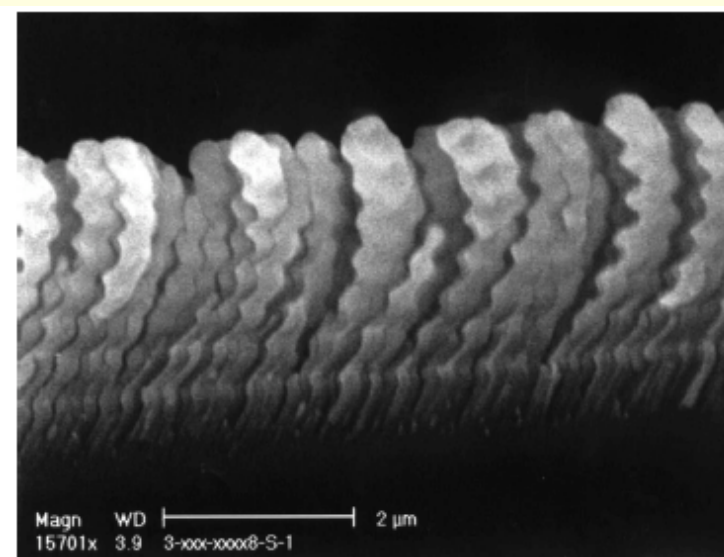
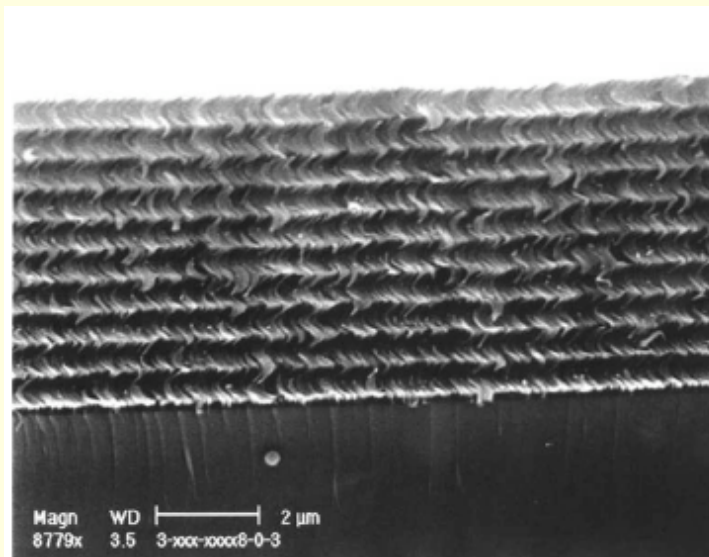
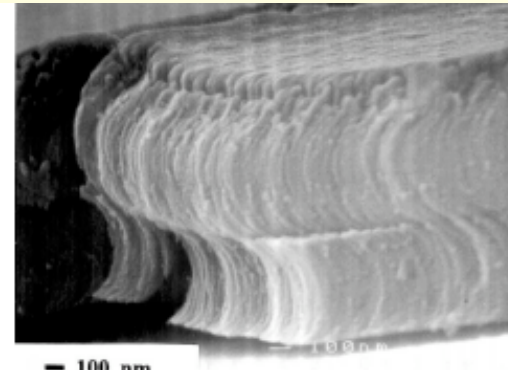
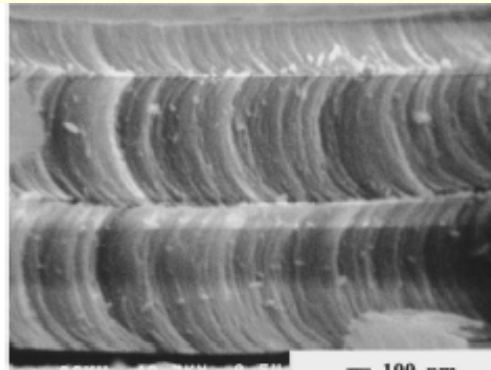
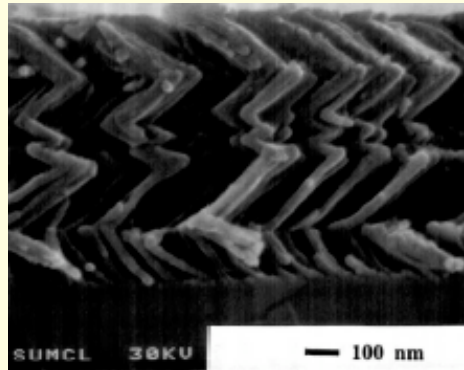
PENNSTATE



A. Lakhtakia

# INTRODUCTION

A. Lakhtakia





# Sculptured Thin Films

Assemblies of Parallel Curved Nanowires/Submicronwires

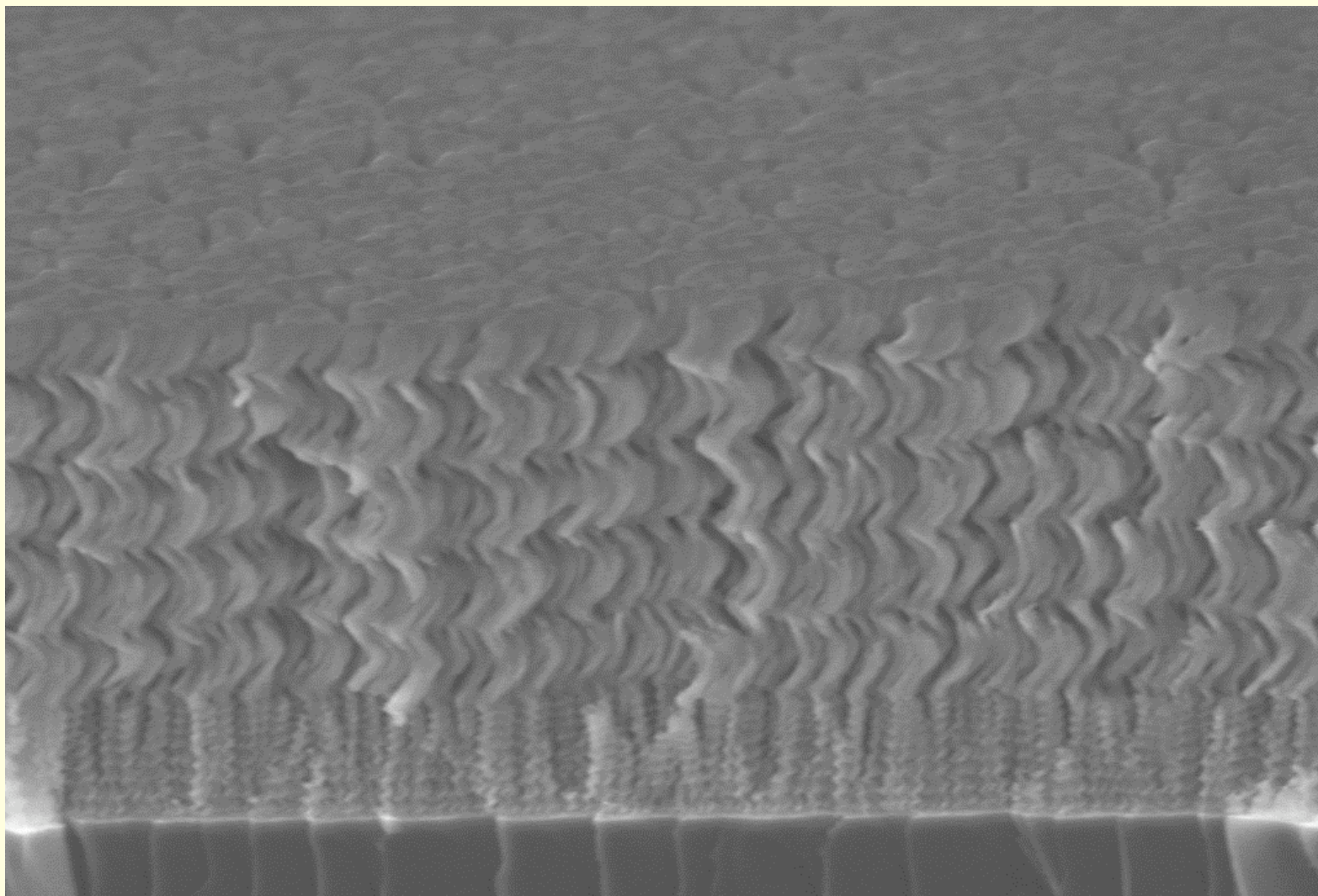
Controllable Nanowire Shape

2-D - nematic

3-D - helicoidal

*combination morphologies*

A. Lakhtakia



Matthew Pickett 1 $\mu$ m  
Mag = 50.00 K X

EHT = 3.00 kV  
WD = 2 mm

Signal A = InLens  
Photo No. = 9684

PSU Nanofab LEO 1530

Time :16:34 Date :1 Jul 2003



# Sculptured Thin Films

Assemblies of Parallel Curved Nanowires/Submicronwires

Controllable Nanowire Shape

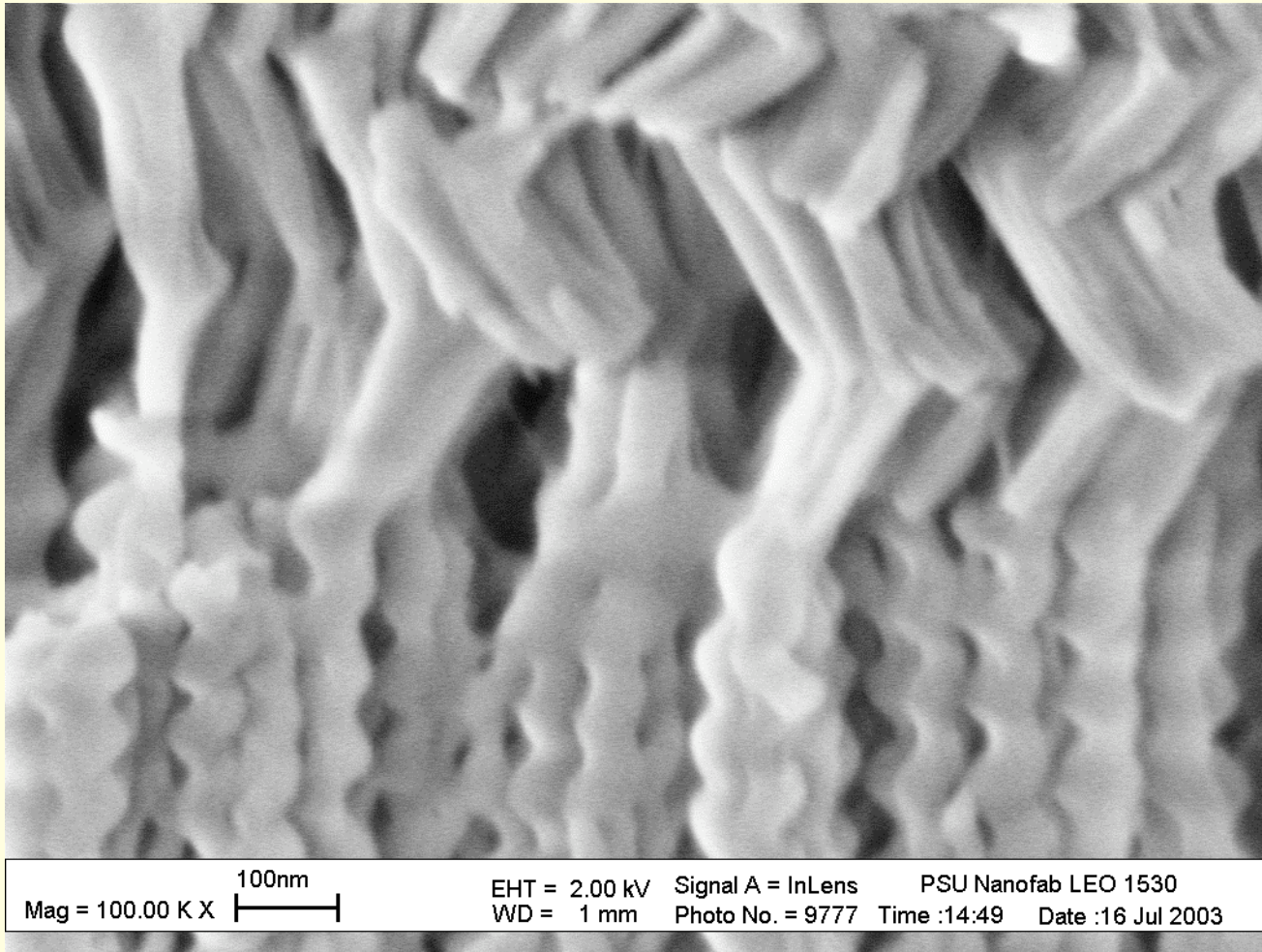
2-D - nematic

3-D - helicoidal

*combination morphologies*

vertical sectioning

A. Lakhtakia







# Sculptured Thin Films

Assemblies of Parallel Curved Nanowires/Submicronwires

Controllable Nanowire Shape

2-D - nematic

3-D - helicoidal

*combination morphologies*

vertical sectioning

Nanoengineered Materials (1-3 nm clusters)

*Controllable Porosity (10-90 %)*



# Sculptured Thin Films

## *Antecedents:*

- (i) Young and Kowal - 1959*
- (ii) Niuewenhuizen & Haanstra - 1966*
- (iii) Motohiro & Taga - 1989*

*Conceptualized by Lakhtakia & Messier (1992-1995)*

*Optical applications (1992- )*

*Biological applications (2003- )*



A. Lakhtakia

# Sculptured Thin Films

## *Collaborators:*

*(i) Weiglhofer, University of Glasgow*

*(ii) Robbie & Brett, University of Alberta*

*(iii) McCall, Imperial College London*

*(iv) Hodgkinson, University of Otago*

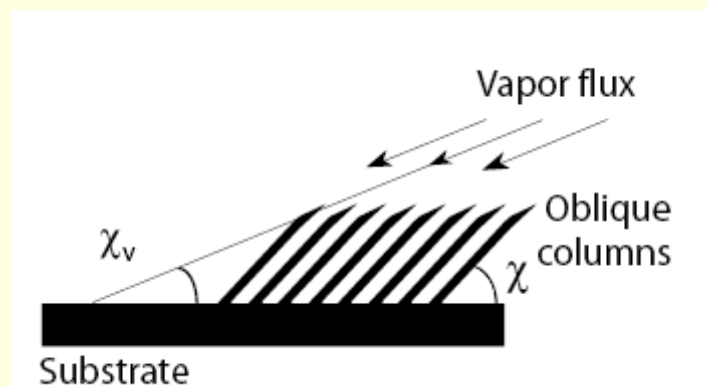
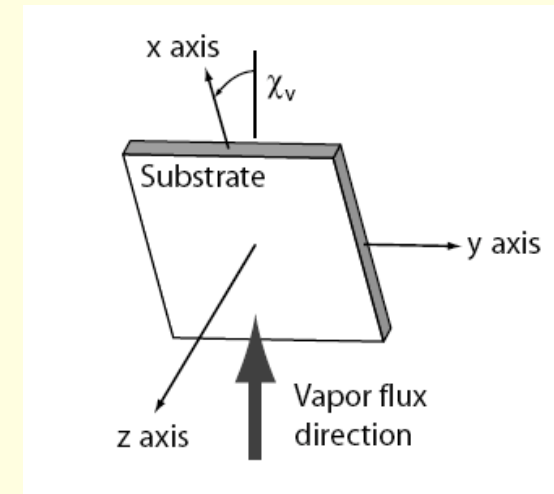
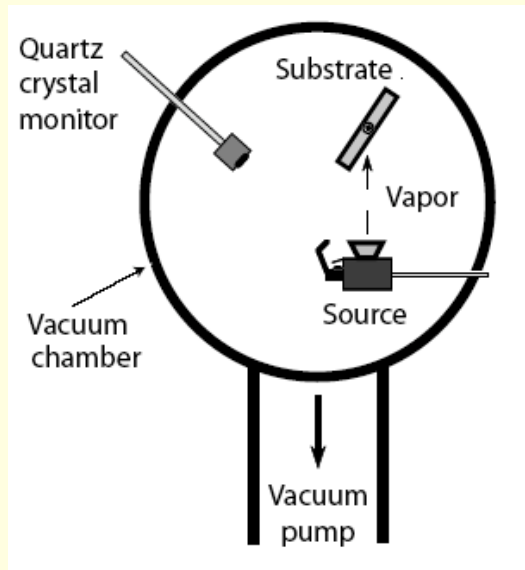
*(v) Polo, Edinboro University*

*(vi) Reyes, UNAM, Mexico*

*(vii) Penn State Colleagues & Students*

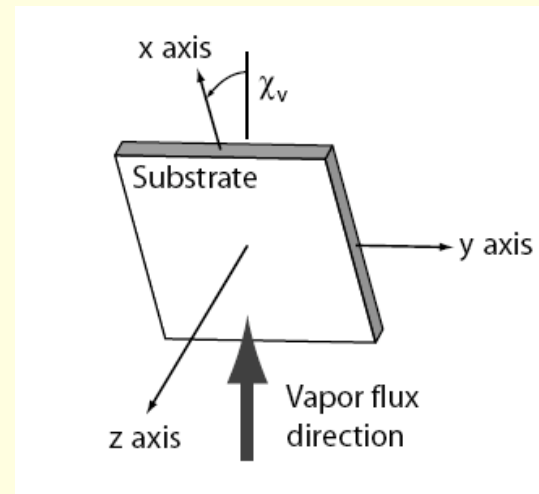
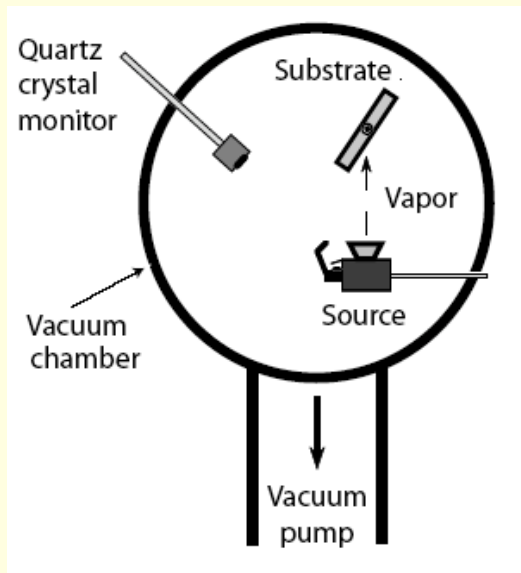
A. Lakhtakia

# Physical Vapor Deposition (Columnar Thin Films)



A. Lakhtakia

# Physical Vapor Deposition (Sculptured Thin Films)



Rotate about  
z axis for  
helicoidal  
morphology

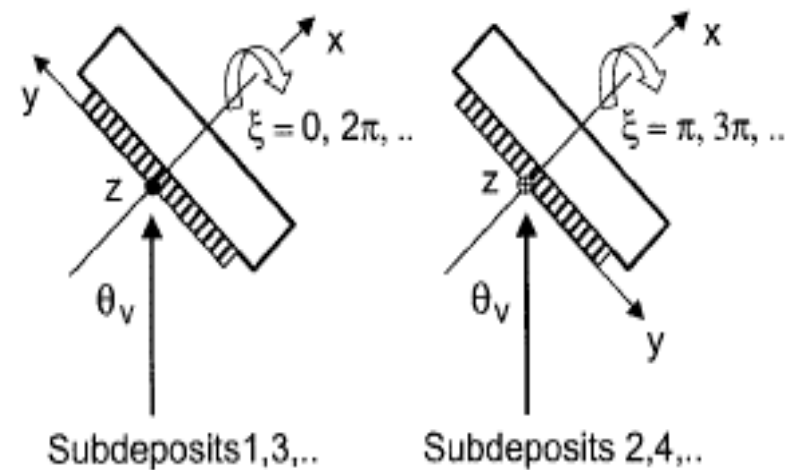
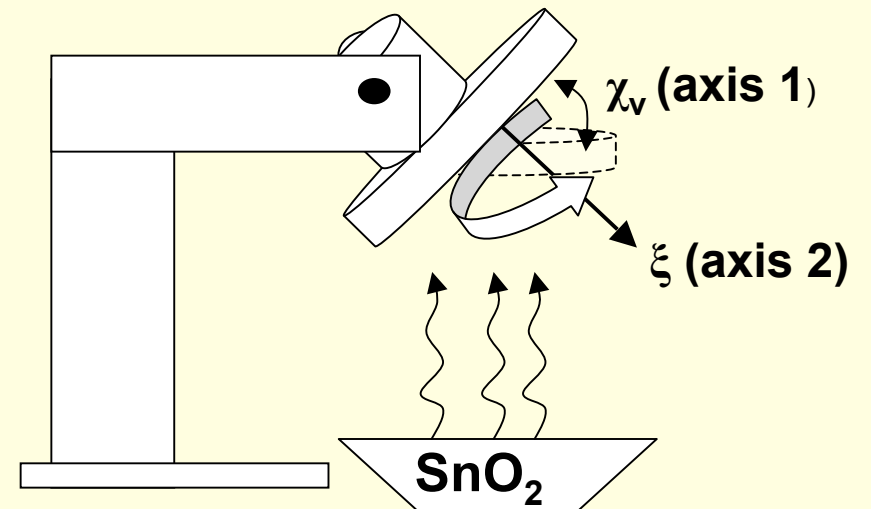
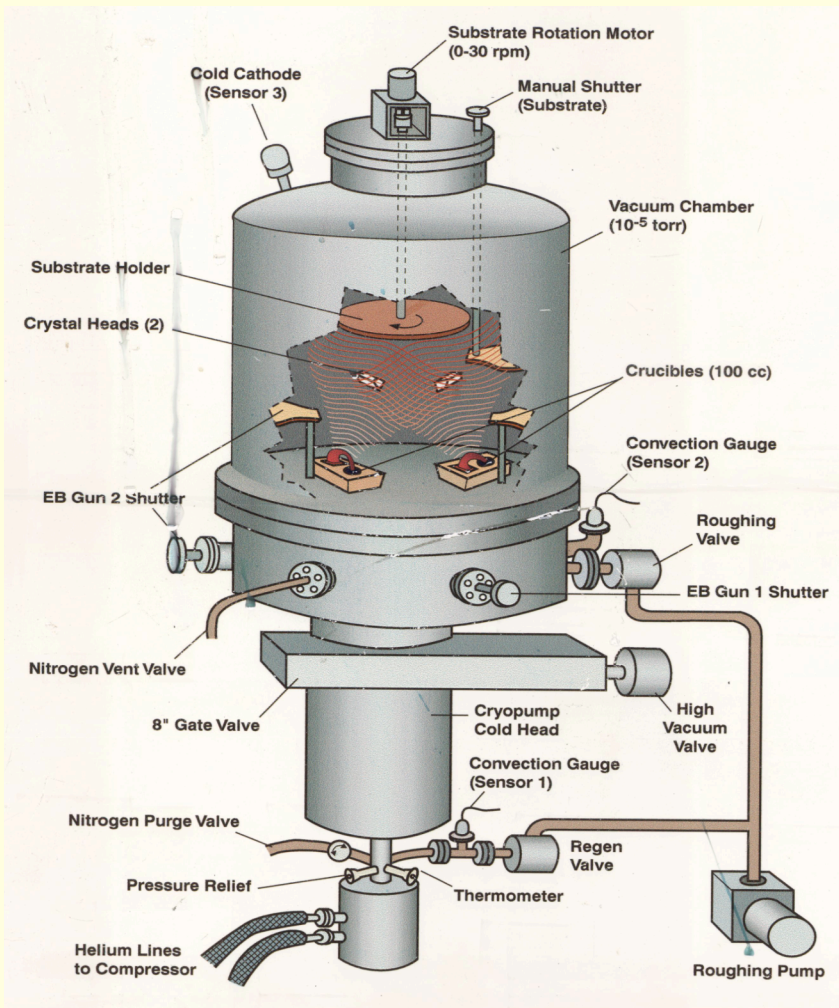
Rotate about  
y axis for  
nematic  
morphology

*Mix and match  
rotations for  
complex  
morphologies*

# Physical Vapor Deposition

A. Lakhtakia

## (Serial Bideposition)



*Adapted for STFs by Hodgkinson*



# Sculptured Thin Films

## Optical Devices:

Polarization Filters  
Bragg Filters  
Ultranarrowband Filters  
Fluid Concentration Sensors  
Bacterial Sensors (Penn State)  
Light Sources (Penn State)

## Biomedical Applications:

Tissue Scaffolds (Penn State)  
Stents (Penn State)  
Bone Repair (Penn State)

## Other Applications:

Photocatalysis (Toyota)  
Thermal Barriers (Alberta)  
Energy Harvesting (Penn State,  
Toledo)

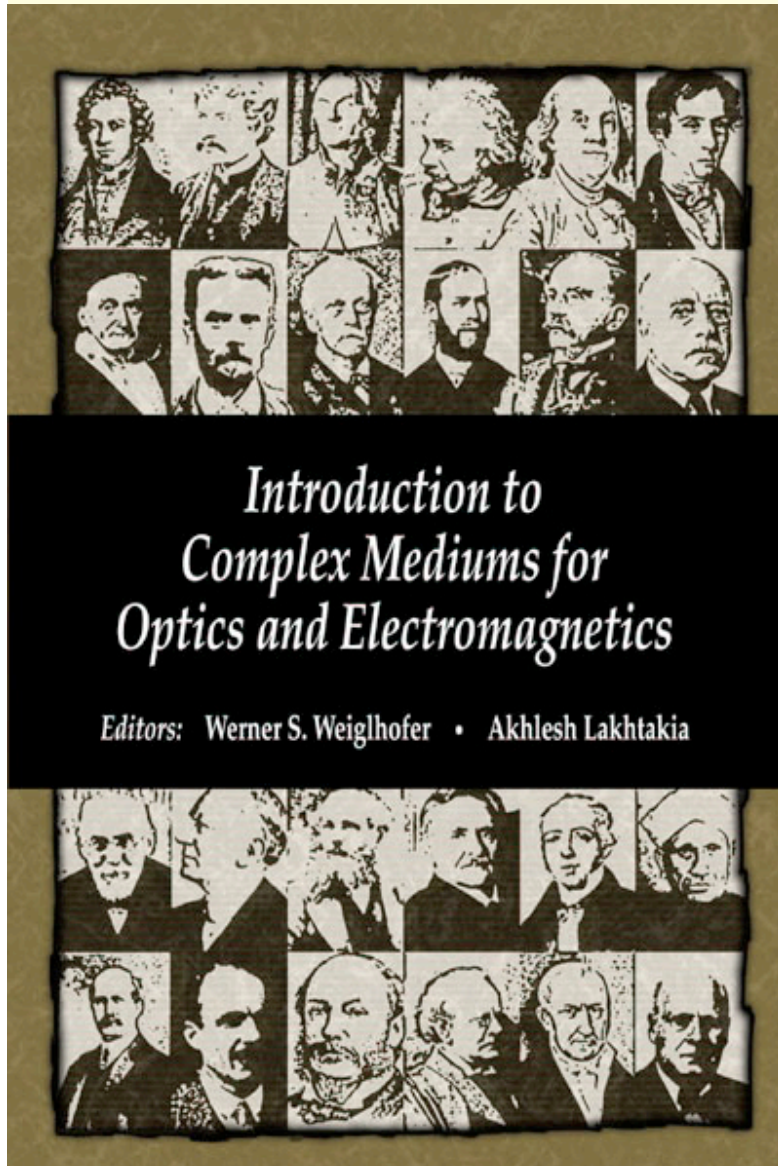


A. Lakhtakia

# OPTICAL MODELING



# Optical Modeling of STFs



Linear  
Bianisotropic  
Materials

SPIE Press (2003)

# Optical Modeling of STFs

$$\begin{aligned} \mathbf{D}(\mathbf{r}, \omega) &= \epsilon_0 \underline{\underline{S}}(z) \cdot \left[ \underline{\underline{\epsilon}}_{ref}(\omega) \cdot \underline{\underline{S}}^T(z) \cdot \mathbf{E}(\mathbf{r}, \omega) \right. \\ &\quad \left. + \underline{\underline{\alpha}}_{ref}(\omega) \cdot \underline{\underline{S}}^T(z) \cdot \mathbf{H}(\mathbf{r}, \omega) \right], \\ \mathbf{B}(\mathbf{r}, \omega) &= \mu_0 \underline{\underline{S}}(z) \cdot \left[ \underline{\underline{\beta}}_{ref}(\omega) \cdot \underline{\underline{S}}^T(z) \cdot \mathbf{E}(\mathbf{r}, \omega) \right. \\ &\quad \left. + \underline{\underline{\mu}}_{ref}(\omega) \cdot \underline{\underline{S}}^T(z) \cdot \mathbf{H}(\mathbf{r}, \omega) \right], \end{aligned}$$

Linear  
Bianisotropic  
Materials



*Introduction to  
Complex Mediums for  
Optics and Electromagnetics*

Editors: Werner S. Weiglhofer • Akhlesh Lakhtakia



$$\begin{aligned} \underline{\underline{S}}_x(z) &= \mathbf{u}_x \mathbf{u}_x + (\mathbf{u}_y \mathbf{u}_y + \mathbf{u}_z \mathbf{u}_z) \cos \xi(z) \\ &\quad + (\mathbf{u}_z \mathbf{u}_y - \mathbf{u}_y \mathbf{u}_z) \sin \xi(z), \\ \underline{\underline{S}}_y(z) &= \mathbf{u}_y \mathbf{u}_y + (\mathbf{u}_x \mathbf{u}_x + \mathbf{u}_z \mathbf{u}_z) \cos \tau(z) \\ &\quad + (\mathbf{u}_z \mathbf{u}_x - \mathbf{u}_x \mathbf{u}_z) \sin \tau(z), \\ \underline{\underline{S}}_z(z) &= \mathbf{u}_z \mathbf{u}_z + (\mathbf{u}_x \mathbf{u}_x + \mathbf{u}_y \mathbf{u}_y) \cos \zeta(z) \\ &\quad + (\mathbf{u}_y \mathbf{u}_x - \mathbf{u}_x \mathbf{u}_y) \sin \zeta(z). \end{aligned}$$

SPIE Press (2003)



# Optical Modeling of STFs

## Dielectric Materials

$$\begin{aligned}\mathbf{D}(\mathbf{r}, \omega) &= \epsilon_0 \underline{\underline{\epsilon}}_r(z, \omega) \cdot \mathbf{E}(\mathbf{r}, \omega) \\ &= \epsilon_0 \underline{\underline{S}}(z) \cdot \underline{\underline{\epsilon}}_{ref}(\omega) \cdot \underline{\underline{S}}^T(z) \cdot \mathbf{E}(\mathbf{r}, \omega), \\ \mathbf{B}(\mathbf{r}, \omega) &= \mu_0 \mathbf{H}(\mathbf{r}, \omega).\end{aligned}$$

# Optical Modeling of STFs

## Locally Orthorhombic Materials

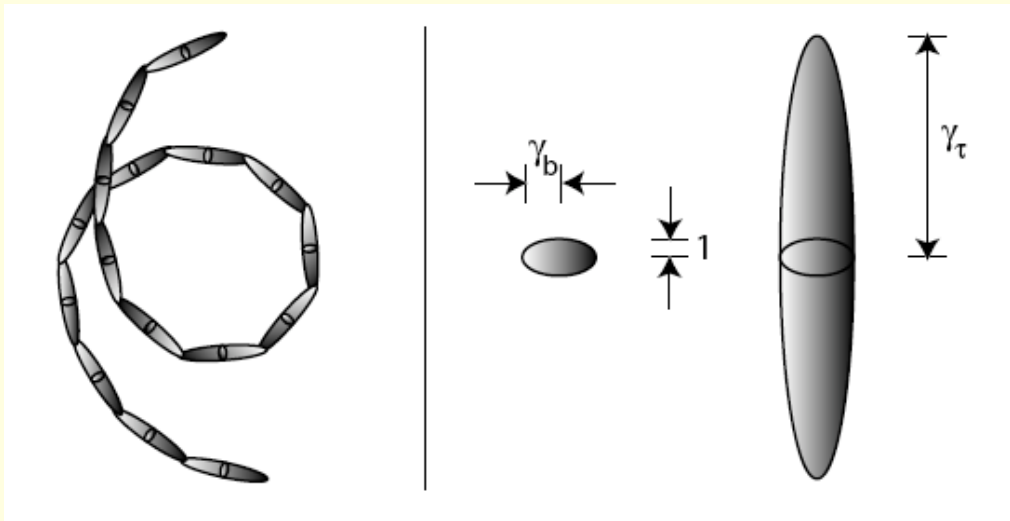
$$\begin{aligned}\mathbf{D}(\mathbf{r}, \omega) &= \epsilon_0 \underline{\underline{\epsilon}}_r(z, \omega) \cdot \mathbf{E}(\mathbf{r}, \omega) \\ &= \epsilon_0 \underline{\underline{S}}(z) \cdot \underline{\underline{\epsilon}}_{ref}(\omega) \cdot \underline{\underline{S}}^T(z) \cdot \mathbf{E}(\mathbf{r}, \omega), \\ \mathbf{B}(\mathbf{r}, \omega) &= \mu_0 \mathbf{H}(\mathbf{r}, \omega).\end{aligned}$$

$$\underline{\underline{\epsilon}}_{ref}(\omega) = \underline{\underline{\hat{S}}}_y(\chi) \cdot \underline{\underline{\epsilon}}_{ref}^o(\omega) \cdot \underline{\underline{\hat{S}}}_y^T(\chi)$$

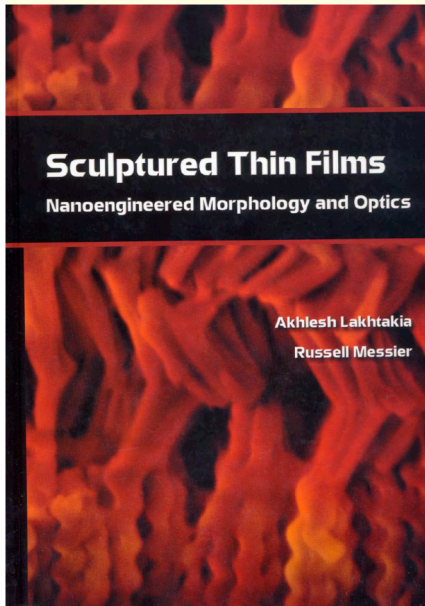
$$\underline{\underline{\epsilon}}_{ref}^o(\omega) = \underline{\underline{\epsilon}}_{ref}(\omega) \Big|_{\chi=0} = \epsilon_a(\omega) \mathbf{u}_z \mathbf{u}_z + \epsilon_b(\omega) \mathbf{u}_x \mathbf{u}_x + \epsilon_c(\omega) \mathbf{u}_y \mathbf{u}_y$$

$$\underline{\underline{\hat{S}}}_y(\chi) = \mathbf{u}_y \mathbf{u}_y + (\mathbf{u}_x \mathbf{u}_x + \mathbf{u}_z \mathbf{u}_z) \cos \chi + (\mathbf{u}_z \mathbf{u}_x - \mathbf{u}_x \mathbf{u}_z) \sin \chi$$

# Optical Modeling of STFs



Homogenize a collection of parallel ellipsoids to get  $\epsilon_{ref}^o(\omega)$



Sherwin and Lakhtakia (2001-2003):  
Bruggeman formalism

Mathematica  
Program

# Optical Modeling of STFs

## Wave Propagation

$$\mathbf{E}(\mathbf{r}, \omega) = \mathbf{e}(z, \kappa, \psi, \omega) \exp [i\kappa(x \cos \psi + y \sin \psi)]$$

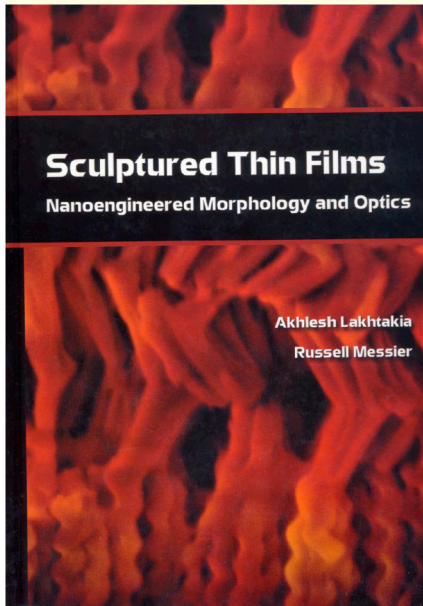
$$\mathbf{H}(\mathbf{r}, \omega) = \mathbf{h}(z, \kappa, \psi, \omega) \exp [i\kappa(x \cos \psi + y \sin \psi)]$$

$$\nabla \times \mathbf{E}(\mathbf{r}, \omega) = i\omega \mathbf{B}(\mathbf{r}, \omega),$$

$$\nabla \times \mathbf{H}(\mathbf{r}, \omega) = -i\omega \mathbf{D}(\mathbf{r}, \omega),$$

$$\frac{d}{dz} [\mathbf{f}(z, \kappa, \psi, \omega)] = i[\mathbf{P}(z, \kappa, \psi, \omega)] [\mathbf{f}(z, \kappa, \psi, \omega)].$$

$$[\mathbf{f}(z, \kappa, \psi, \omega)] = \begin{bmatrix} e_x(z, \kappa, \psi, \omega) \\ e_y(z, \kappa, \psi, \omega) \\ h_x(z, \kappa, \psi, \omega) \\ h_y(z, \kappa, \psi, \omega) \end{bmatrix}$$



Mathematica  
Program

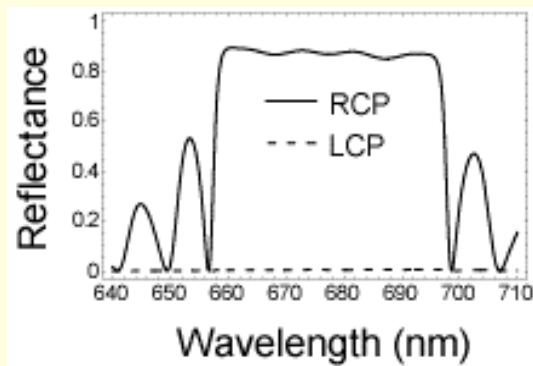
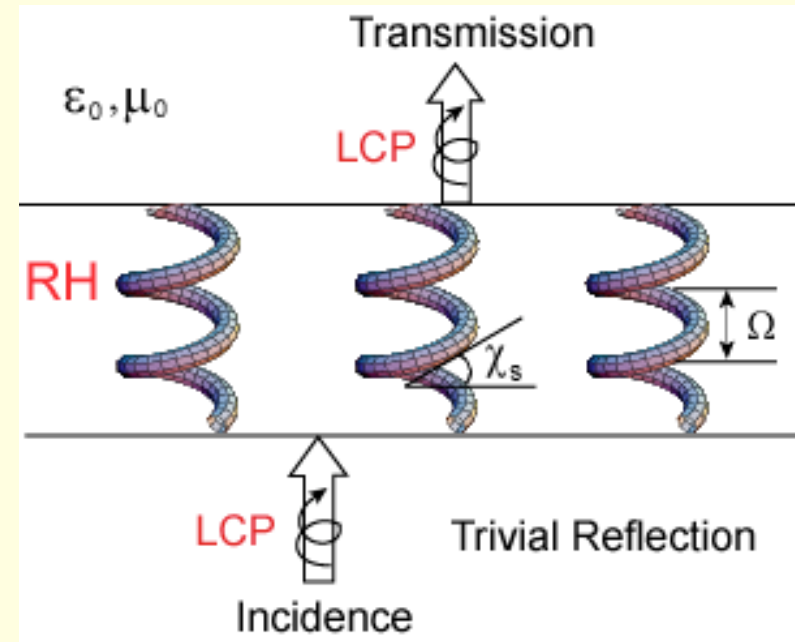
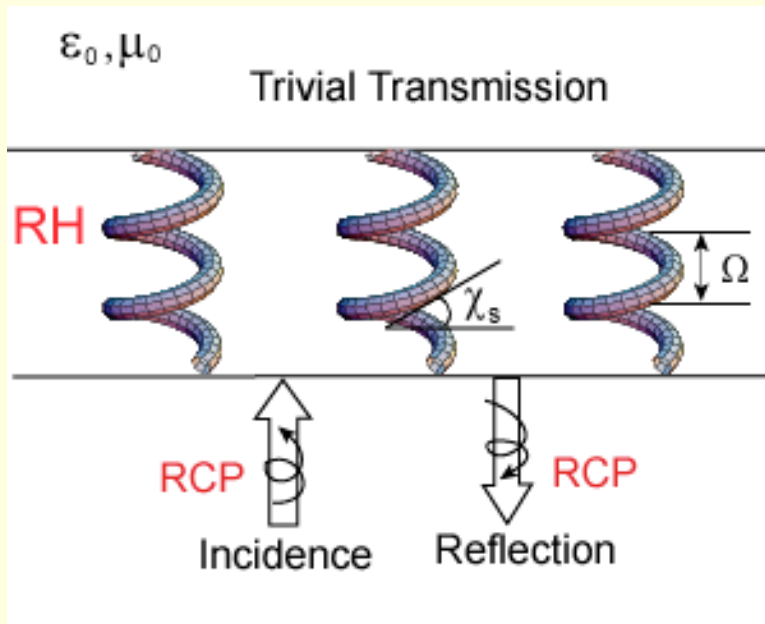
PENNSYLVANIA STATE UNIVERSITY



A. Lakhtakia

# EXAMPLES OF POLARIZATION ENGINEERING

# Chiral STFs: Circular Bragg Phenomenon



A simple explanation (Coupled-Wave Theory):

- Co-handed wave: Scalar Bragg grating
- Cross-handed wave: Homogeneous bulk medium



# Chiral STF as CP Filter

442. J.A. Sherwin, A. Lakhtakia & I.J. Hodgkinson, 'On calibration of a nominal structure--property relationship model for chiral sculptured thin films by axial transmittance measurements,' *Optics Communications*, **209**, 2002, 369–375.

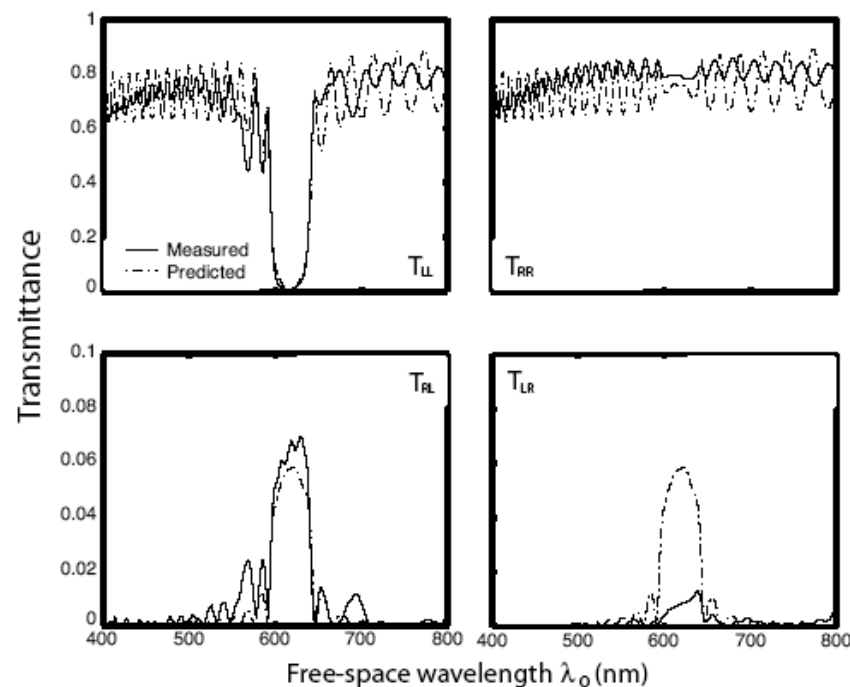


Figure 10.2: Predicted and measured transmittances of a circular polarization filter as functions of the free-space wavelength  $\lambda_0$  for normal incidence. The filter is a chiral STF of patinal titanium oxide. The reference permittivity dyadic was predicted with  $\epsilon_s = 6.3 + i0.012$ ,  $\epsilon_v = 1$ ,  $f_v = 0.421$ ,  $\gamma_\tau^{(s)} = \gamma_\tau^{(v)} = 20$ , and  $\gamma_b^{(s)} = \gamma_b^{(v)} = 1.06$  set in Program 6.1. The other parameters are  $\chi = 47$  deg,  $h = -1$ ,  $\Omega = 173$  nm,  $L = 30\Omega$ , and  $\psi = 0$  deg. (Adapted from Sherwin et al. [109] with permission of Elsevier.)



# Chiral STF as CP Filter

## Engineering of Bragg Regime and CP State

$$\underline{\underline{\epsilon}}_{chiral}(z, \omega) = \underline{\underline{S}}_z(z) \cdot \underline{\underline{S}}_y(\chi) \cdot [\epsilon_a(\omega) \hat{u}_z \hat{u}_z + \epsilon_b(\omega) \hat{u}_x \hat{u}_x + \epsilon_c(\omega) \hat{u}_y \hat{u}_y] \cdot \underline{\underline{S}}_y^{-1}(\chi) \cdot \underline{\underline{S}}_z^{-1}(z)$$

$$\underline{\underline{S}}_z(z) = (\hat{u}_x \hat{u}_x + \hat{u}_y \hat{u}_y) \cos(\pi z / \Omega) + h(\hat{u}_y \hat{u}_x - \hat{u}_x \hat{u}_y) \sin(\pi z / \Omega) + \hat{u}_z \hat{u}_z$$

$$\underline{\underline{S}}_y(\chi) = \hat{u}_y \hat{u}_y + (\hat{u}_x \hat{u}_x + \hat{u}_z \hat{u}_z) \cos \chi + (\hat{u}_z \hat{u}_x - \hat{u}_x \hat{u}_z) \sin \chi$$



# Chiral STF as CP Filter

## Engineering of Bragg Regime and CP State

$$\underline{\underline{\epsilon}}_{chiral}(z, \omega) = \underline{\underline{S}}_z(z) \cdot \underline{\underline{S}}_y(\chi) \cdot [\epsilon_a(\omega) \hat{u}_z \hat{u}_z + \epsilon_b(\omega) \hat{u}_x \hat{u}_x + \epsilon_c(\omega) \hat{u}_y \hat{u}_y] \cdot \underline{\underline{S}}_y^{-1}(\chi) \cdot \underline{\underline{S}}_z^{-1}(z)$$

$$\underline{\underline{S}}_z(z) = (\hat{u}_x \hat{u}_x + \hat{u}_y \hat{u}_y) \cos(\pi z / \Omega) + h(\hat{u}_y \hat{u}_x - \hat{u}_x \hat{u}_y) \sin(\pi z / \Omega) + \hat{u}_z \hat{u}_z$$

$$\underline{\underline{S}}_y(\chi) = \hat{u}_y \hat{u}_y + (\hat{u}_x \hat{u}_x + \hat{u}_z \hat{u}_z) \cos \chi + (\hat{u}_z \hat{u}_x - \hat{u}_x \hat{u}_z) \sin \chi$$

Rotational Speed: Controls  $\Omega$

Rotational Sense: Controls  $h$

Vapor Incidence Angle: Controls  $\epsilon_{a,b,c}$  and  $\chi$

# Chiral STF as CP Filter

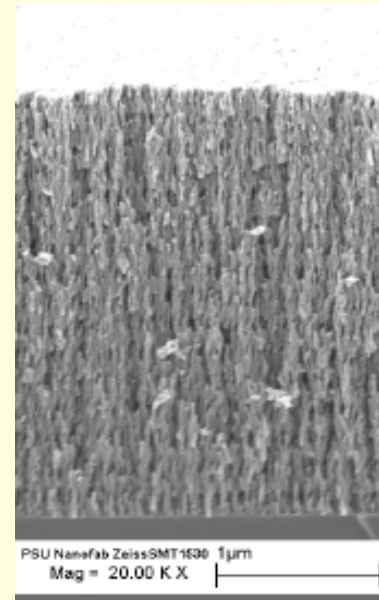
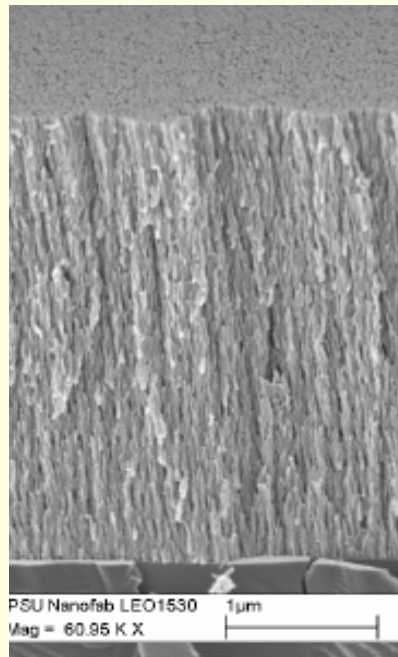
## Post-Deposition Engineering of Bragg Regime

558. S.M. Pursel, M.W. Horn & **A. Lakhtakia**, Blue-shifting of circular Bragg phenomenon by annealing of chiral sculptured thin films, *Optics Express*, **14**, 2006, 8001 – 8012.

### Annealing

*before*

*after*



# Chiral STF as CP Filter

## Post-Deposition Engineering of Bragg Regime

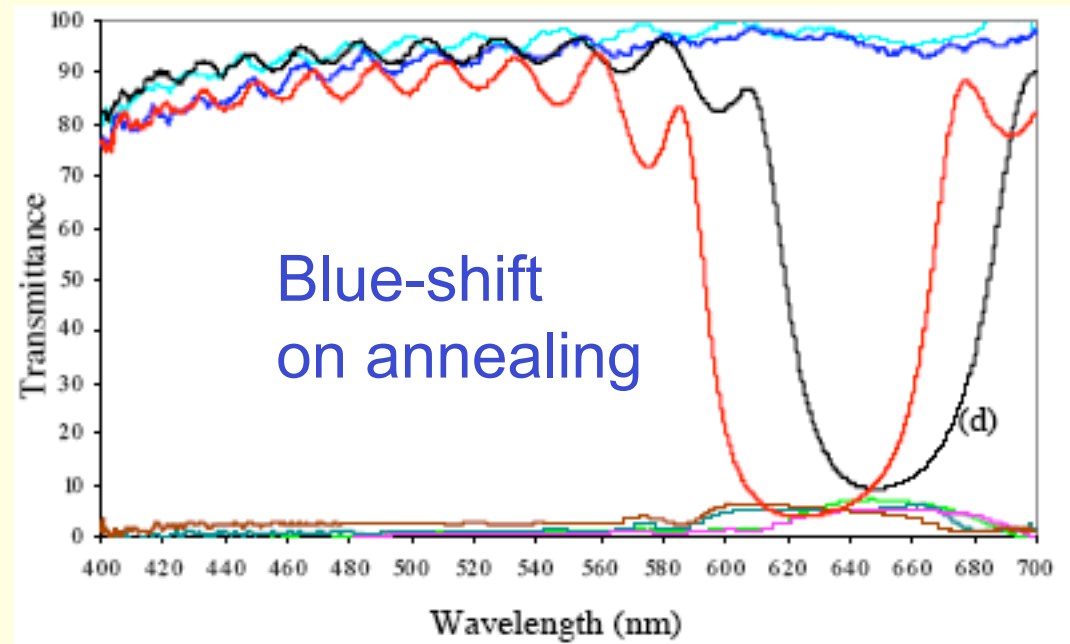
### Annealing

#### Blue-shift factors:

- (i) Decreases pitch
- (ii) Thins nanowires

#### Red-shift factors:

- (i) Increases permittivity



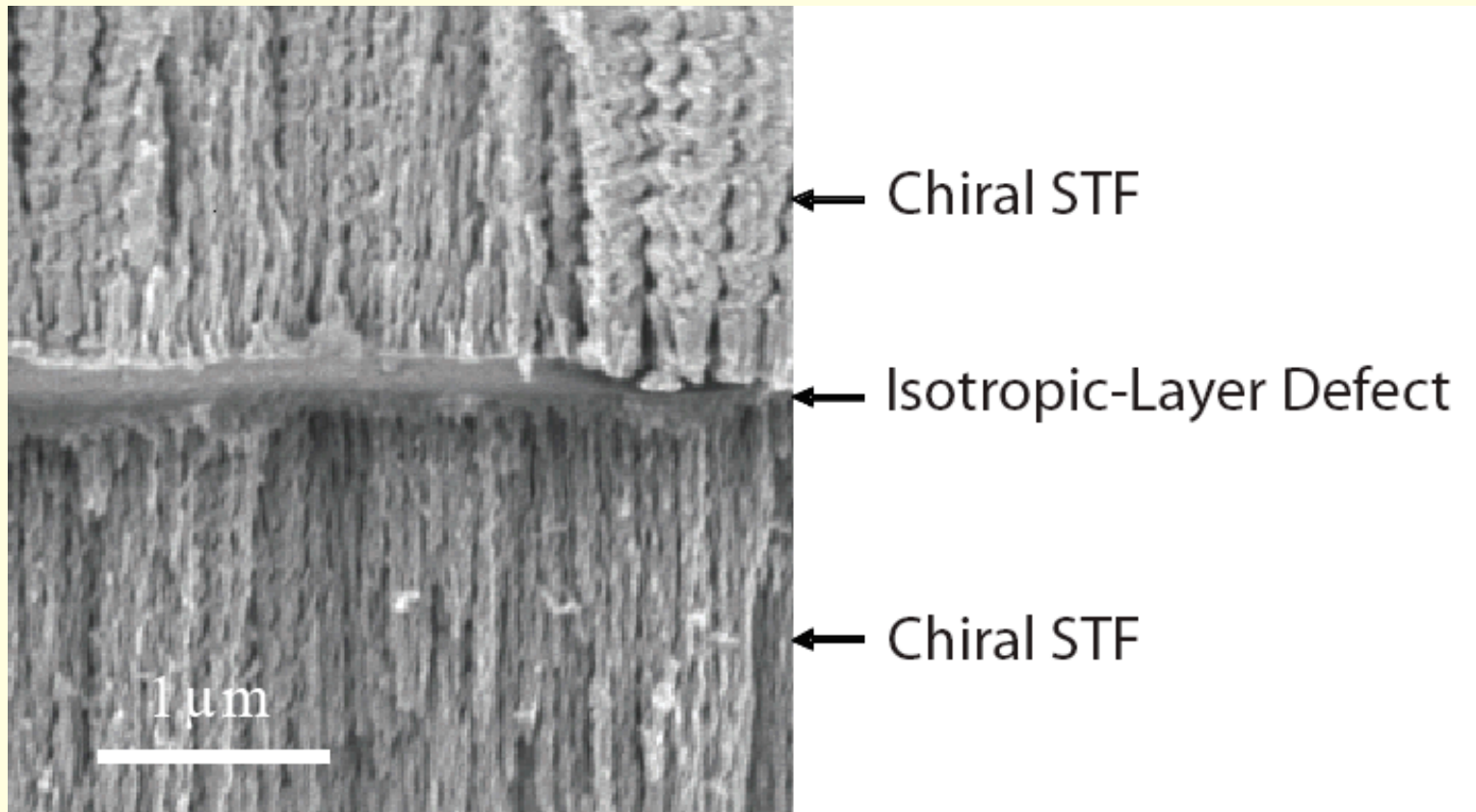


# Spectral Hole Filter

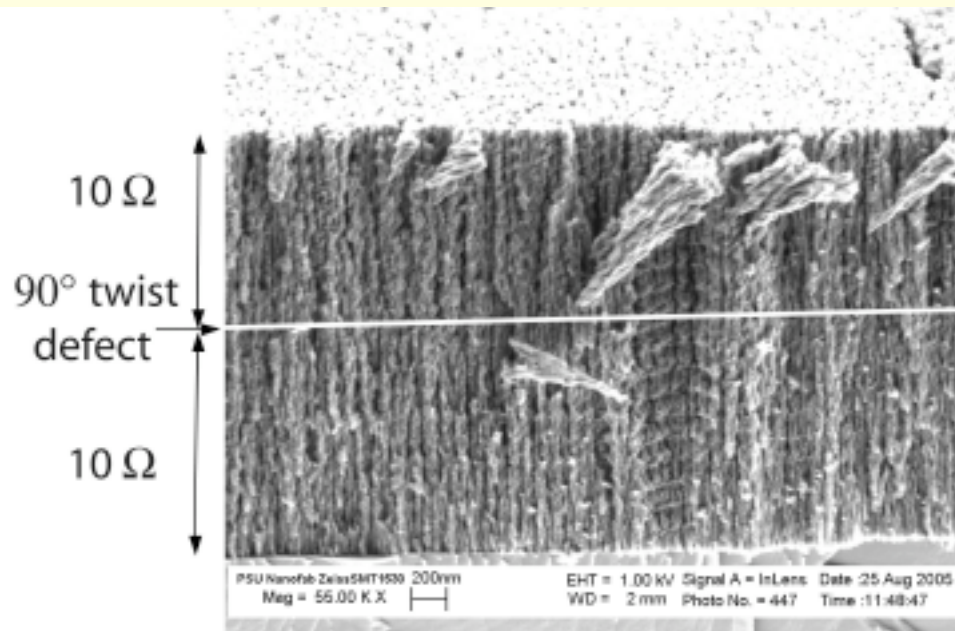
## Central Phase Defect in a Chiral STF

- Homogeneous-layer defect
  - *Isotropic*
  - *Anisotropic*
- Twist defect
- Structurally-chiral-layer defect

# Spectral Hole Filter

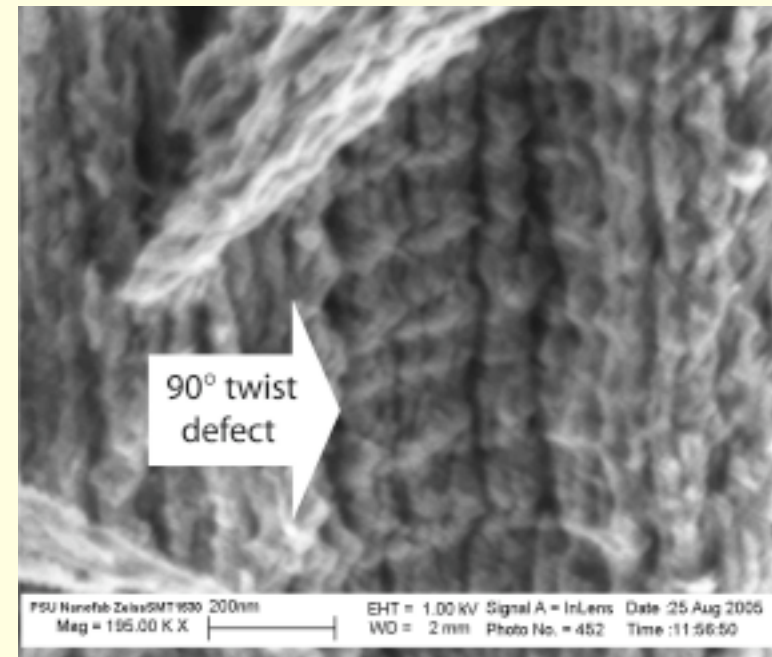
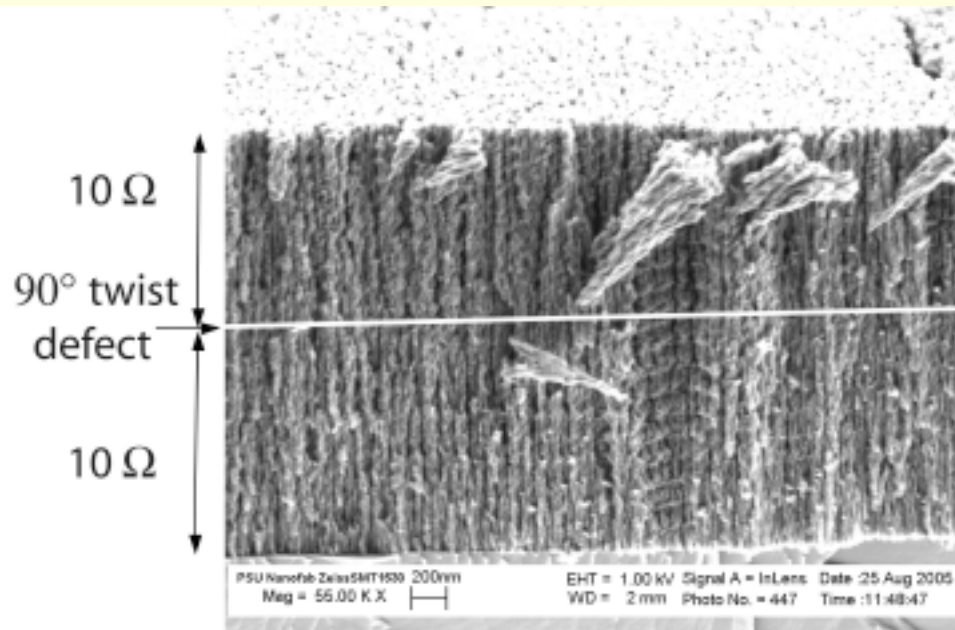


# Spectral Hole Filter



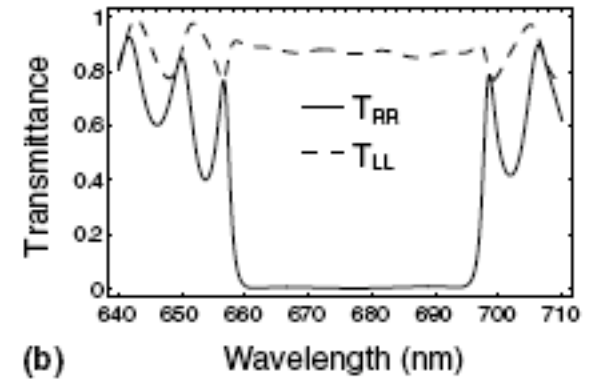
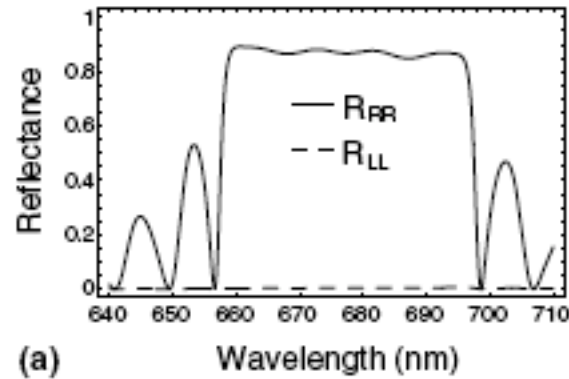


# Spectral Hole Filter



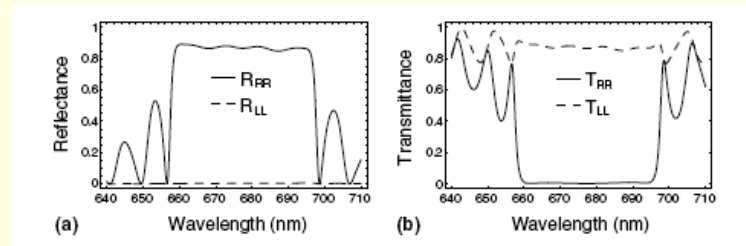
# Spectral Hole Filter

Defect-free

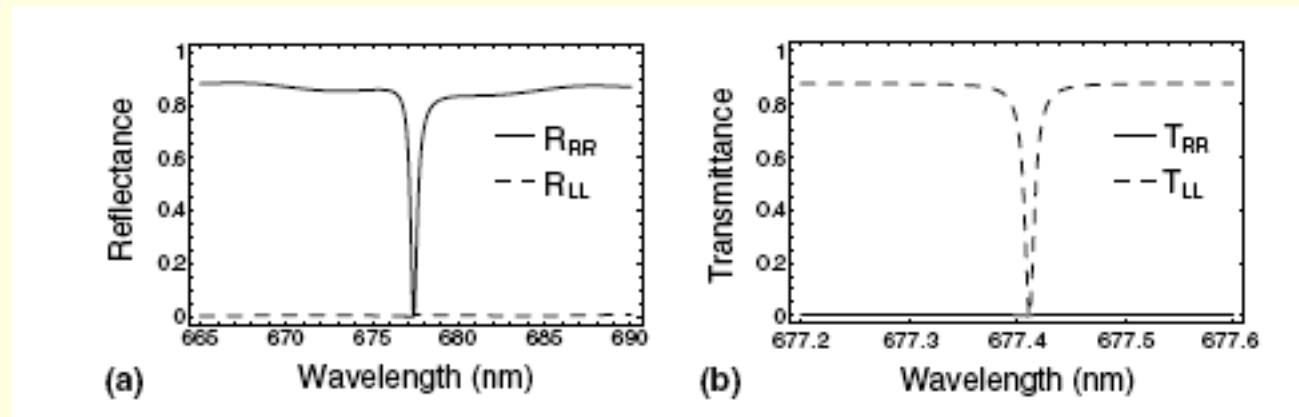


# Spectral Hole Filter

Defect-free



With defect



Thin Chiral STF  
Reflection Hole  
Co-handed  
Theory/Experiment

Thick Chiral STF  
Transmission Hole  
Cross-handed  
Theory only

# Spectral Hole Filter

## Isotropic-layer defect

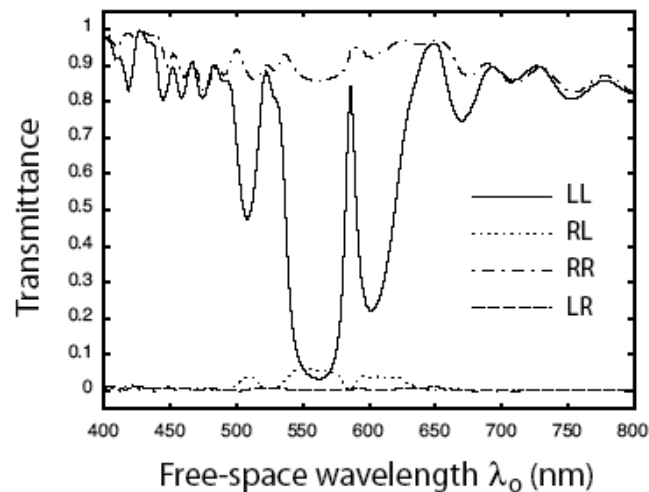


Figure 10.10: Measured transmittances of a narrow bandpass filter comprising an isotropic homogeneous spacer of hafnium oxide interposed between two identical, structurally left-handed, chiral STF sections of titanium oxide. Evidence of a hole in the spectrum of  $R_{LL}$  at 580-nm wavelength is provided by the spectrum of  $T_{LL}$ . (Adapted from Hodgkinson et al. [125] with permission of Elsevier.)

# Spectral Hole Filter

Twist defect

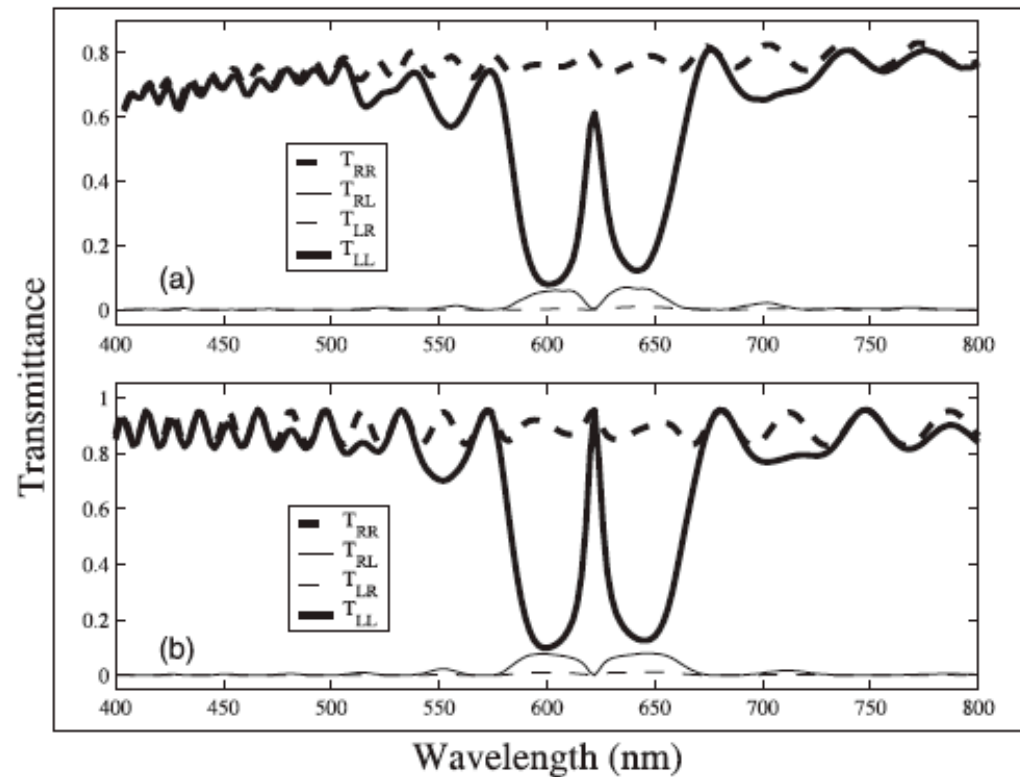


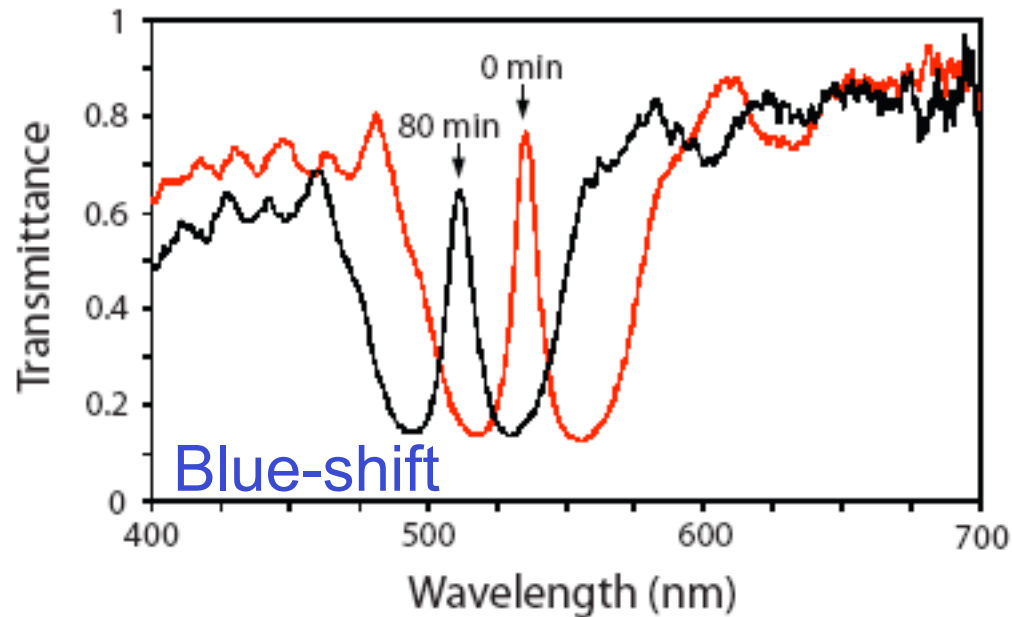
Fig. 7. (a) Measured spectra of the transmittances,  $T_{RR}$ ,  $T_{RL}$ ,  $T_{LR}$  and  $T_{LL}$  of the spacerless filter sp290200 with twist  $\psi_t = 90^\circ$ . (b) Transmittance spectrums simulated for the above filter using the parameters  $h = -1$ ,  $N = 6$ ,  $\Omega = 163$  nm,  $n_{av} = 1.914$  and  $\Delta n = 0.116$ , so that  $\lambda_0^{Br} = 622$  nm.

388. I.J. Hodgkinson, Q.h. Wu, K.E. Thorn, A. Lakhtakia & M.W. McCall, 'Spacerless circular-polarization spectral-hole filters using chiral sculptured thin films: theory and experiment,' *Optics Communications*, **184**, 2000, 57–66.

# Spectral Hole Filter

## Post-Deposition Engineering

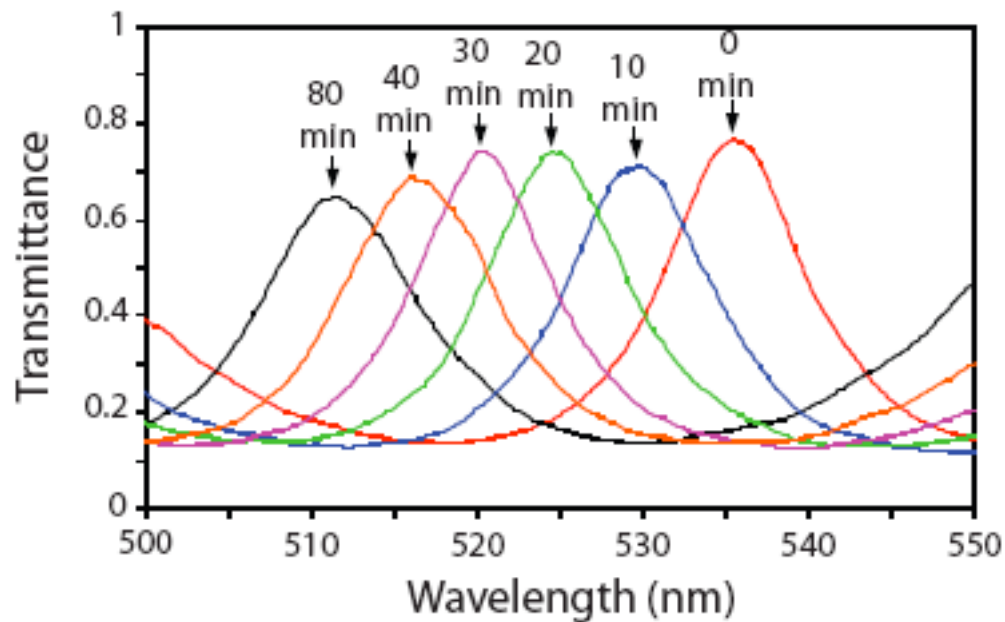
### Chemical Etching



# Spectral Hole Filter

## Post-Deposition Engineering

### Chemical Etching Columnar Thinning Blue Shift



# Fluid Concentration Sensor

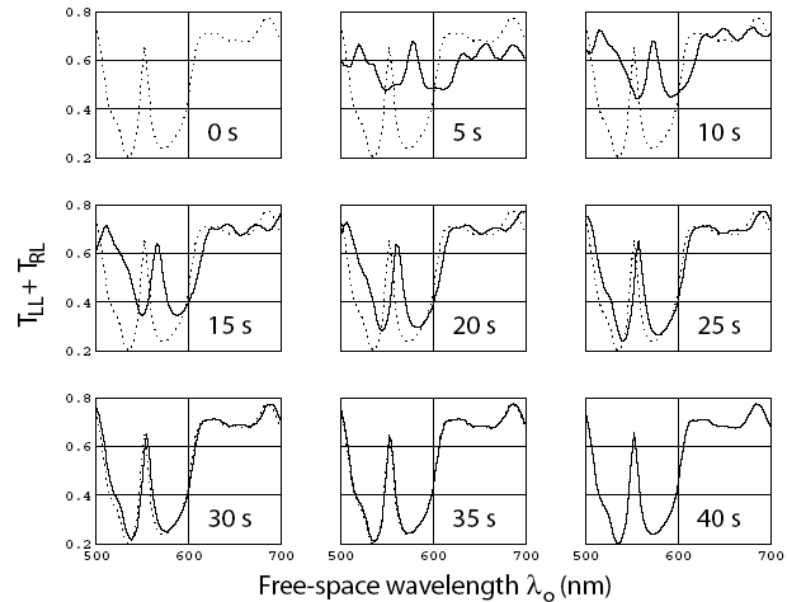


Figure 10.22: Optical response of a narrow bandpass filter, described by Eq. (10.17) and made of two structurally left-handed chiral STF sections, on infiltration by water vapor. The dotted lines indicate the measured transmittance spectrum when the filter was dry. The filter was flooded with water and then allowed to recover by evaporation in air. Transmittance spectra recorded at 5-s intervals after the flooding are shown. (Adapted from Lakhtakia et al. [105] with permission of Elsevier.)

410. **A. Lakhtakia**, M.W. McCall, J.A. Sherwin, Q.H. Wu & I.J. Hodgkinson, 'Sculptured-thin-film spectral holes for optical sensing of fluids,' *Optics Communications*, **194**, 2001, 33–46.





A. Lakhtakia

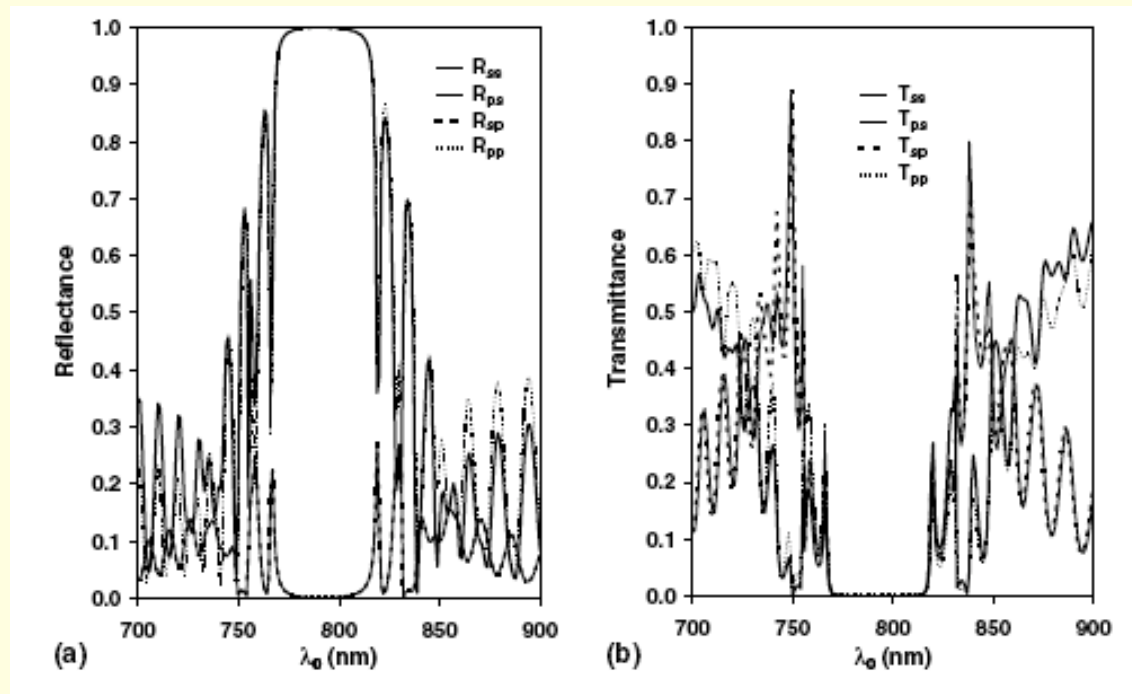
# MORE EXAMPLES OF POLARIZATION ENGINEERING

# Tilt-Modulated Chiral STF

$$\underline{\underline{\epsilon}}_{tmc}(z, \omega) = \underline{\underline{S}}_z(z) \cdot \underline{\underline{S}}_y[\chi(z)] \cdot [\epsilon_a(z, \omega) \hat{\mathbf{u}}_z \hat{\mathbf{u}}_z + \epsilon_b(z, \omega) \hat{\mathbf{u}}_x \hat{\mathbf{u}}_x + \epsilon_c(z, \omega) \hat{\mathbf{u}}_y \hat{\mathbf{u}}_y] \cdot \underline{\underline{S}}_y^{-1}[\chi(z)] \cdot \underline{\underline{S}}_z^{-1}(z)$$

$$\chi_v(z) = \tilde{\chi}_v + \delta_v \sin(2\pi z / \Omega)$$

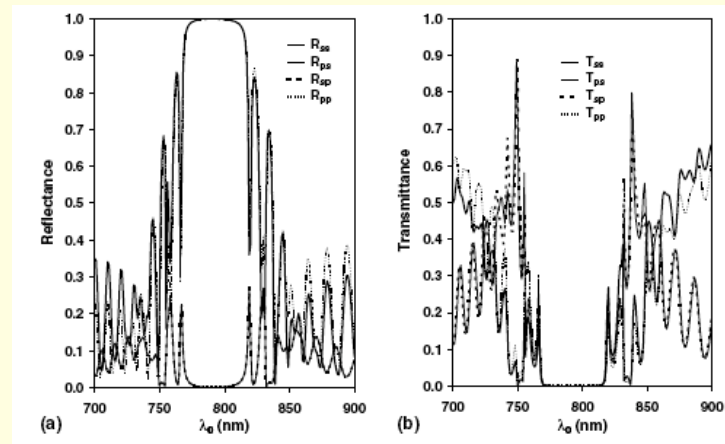
$$\delta_v = 10^\circ, \tilde{\chi}_v = 35^\circ$$



500. J.A. Polo, Jr. & A. Lakhtakia, 'Tilt-modulated chiral sculptured thin films: an alternative to quarter-wave stacks,' *Optics Communications*, **242**, 2004, 13 – 21.

# Tilt-Modulated Chiral STF

## Ordinary Dielectric Mirror



### *Advantages:*

(1) Single material

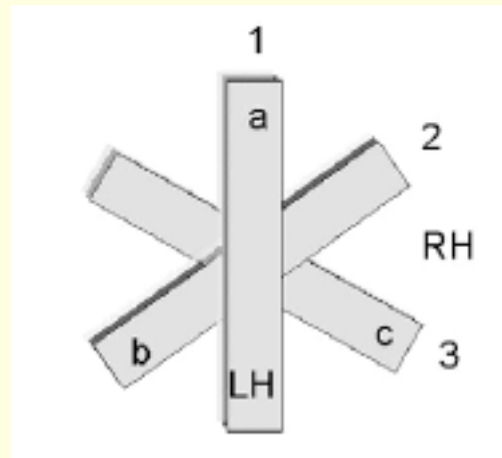
(2) Bragg FWHM governed by tilt-modulation amplitude

# Ambichiral STF

Reusch 1869

$$\underline{\underline{\epsilon}}_n(\omega) = \underline{\underline{R}}_z \left[ 2h \frac{(n-1)\pi}{N} \right] \cdot \underline{\underline{S}}_y(\chi) \cdot [\epsilon_a(\omega) \hat{u}_z \hat{u}_z + \epsilon_b(\omega) \hat{u}_x \hat{u}_x + \epsilon_c(\omega) \hat{u}_y \hat{u}_y] \cdot \underline{\underline{S}}_y^{-1}(\chi) \cdot \underline{\underline{R}}_z^{-1} \left[ 2h \frac{(n-1)\pi}{N} \right] \quad (1)$$

$$\underline{\underline{R}}_z(\zeta) = (\hat{u}_x \hat{u}_x + \hat{u}_y \hat{u}_y) \cos \zeta + (\hat{u}_y \hat{u}_x - \hat{u}_x \hat{u}_y) \sin \zeta + \hat{u}_z \hat{u}_z$$



$$d_n = d_1 \left\{ 1 + a \sin \left[ 4 \frac{(n-1)\pi}{N} \right] \right\}, \quad 0 \leq a \leq 1$$

# Ambichiral STF

All layers of equal thickness.

2 Bragg regimes

Different CP states reflected

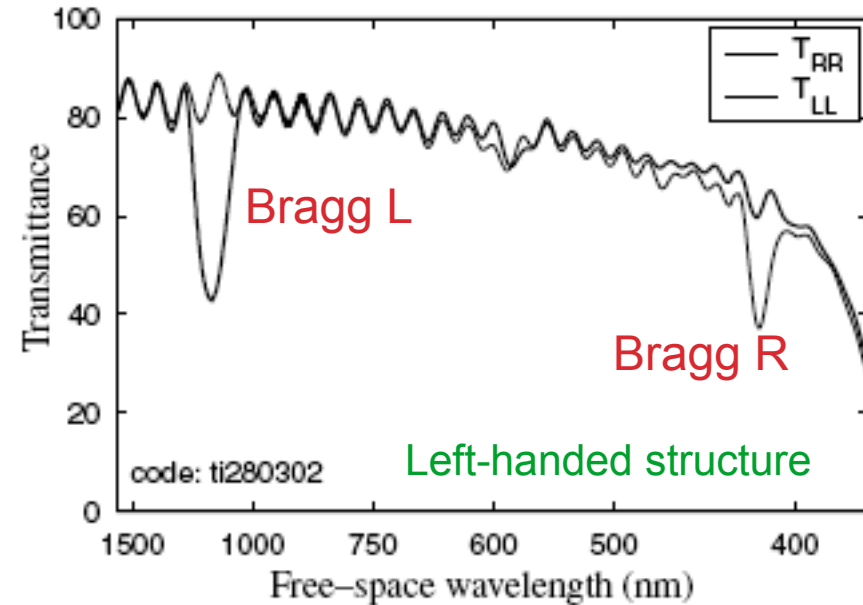


Fig. 4. Measured co-polarized transmittances of an ambichiral layered structure characterized by  $h = -1$ ,  $N = 10q$ , and  $q = 4$ . This structure of titanium oxide was created using the serial bideposition technique.



# Ambichiral STF

Layers of  
unequal thickness.

$$d_n = d_1 \left\{ 1 + a \sin \left[ 4 \frac{(n-1)\pi}{N} \right] \right\}, \quad 0 \leq a \leq 1$$

## 1 Bragg regime

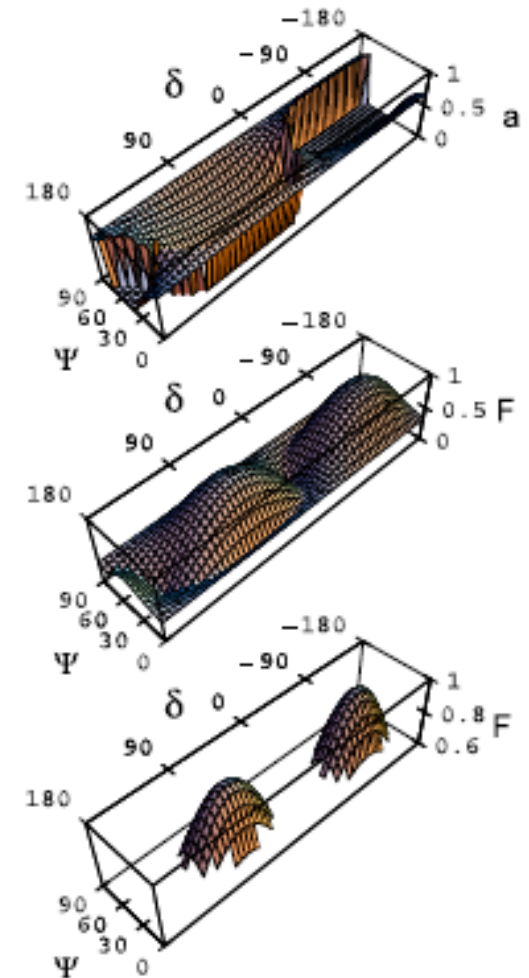
# Ambichiral STF

Layers of  
unequal thickness.

1 Bragg regime

EP states ( $\Psi$  and  $\delta$ ) reflected

Better for CP and nearly CP states



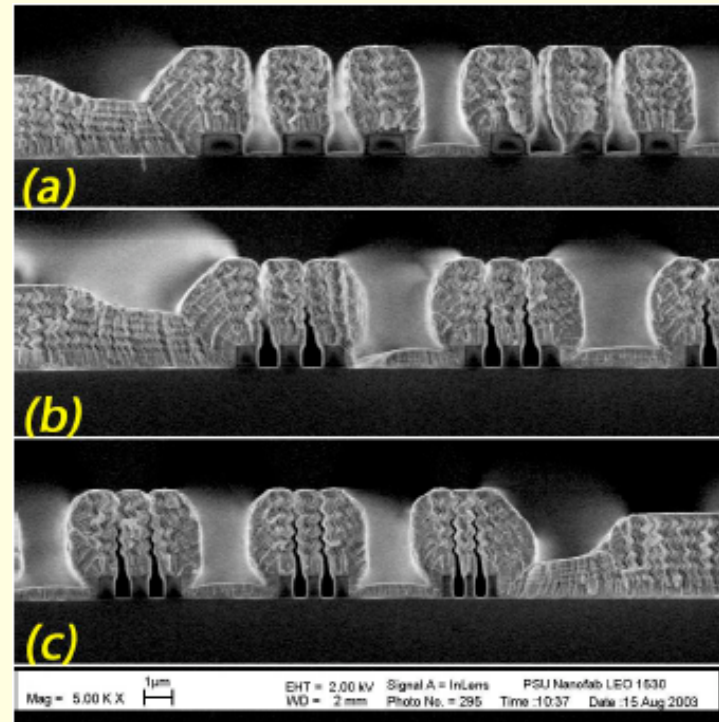
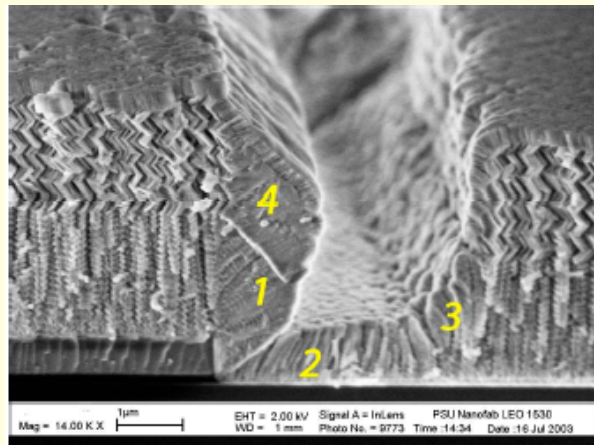
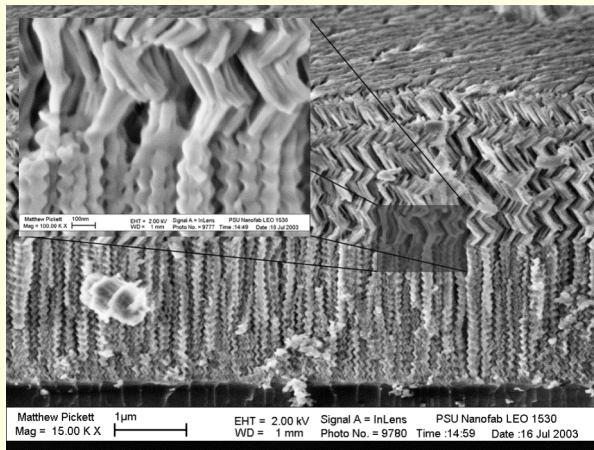
WHAT'S NEXT?



A. Lakhtakia

# STFs WITH TRANSVERSE ARCHITECTURE

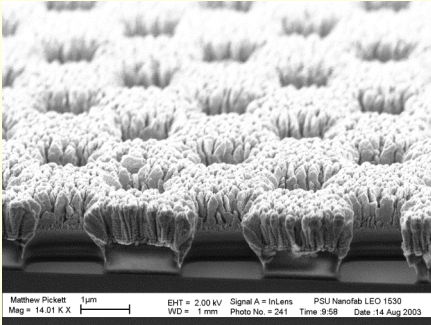
## STFs on Microscale Topography (Cross-sectional SEMs of SiO<sub>x</sub> STFs)



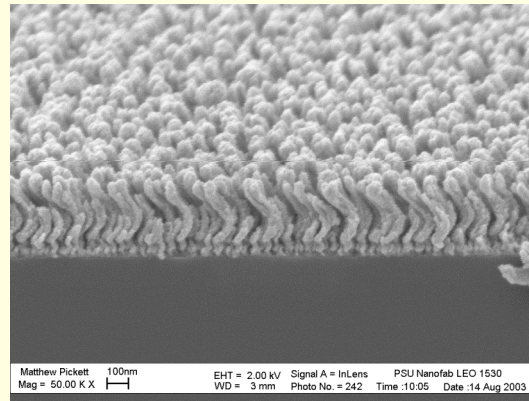
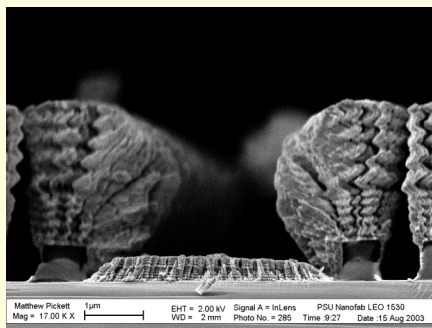
A. Lakhtakia

# STFs WITH TRANSVERSE ARCHITECTURE

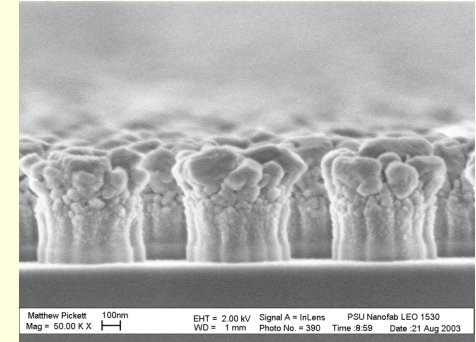
## Metal STFs on Topography



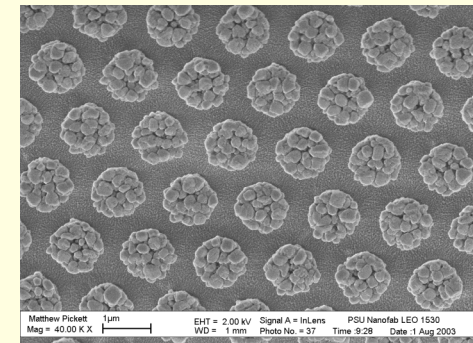
**Chromium**



**Molybdenum**



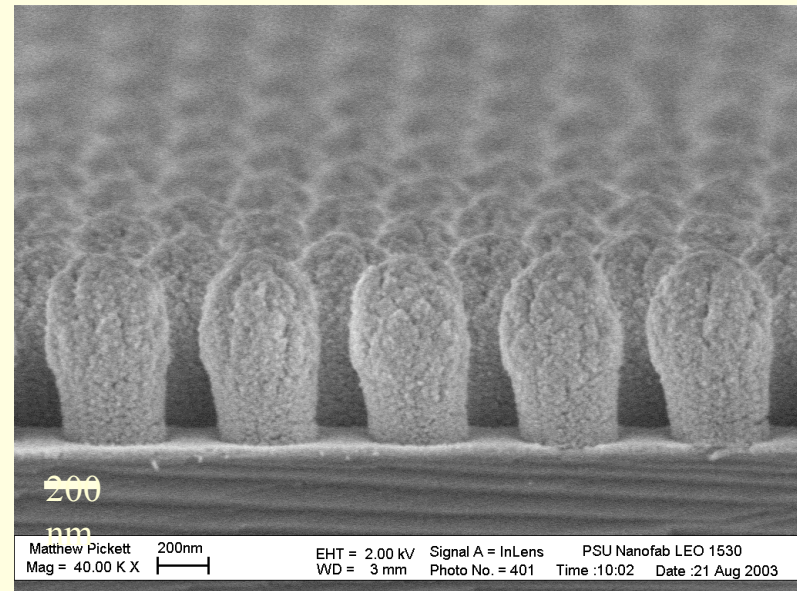
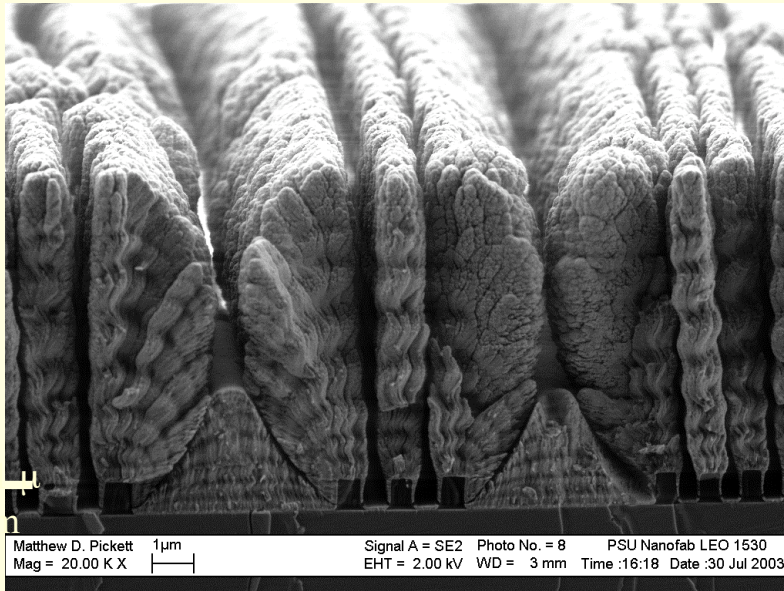
**Aluminum**



A. Lakhtakia

# STFs WITH TRANSVERSE ARCHITECTURE

## Semiconductor STFs on Micro and Nanoscale Topography

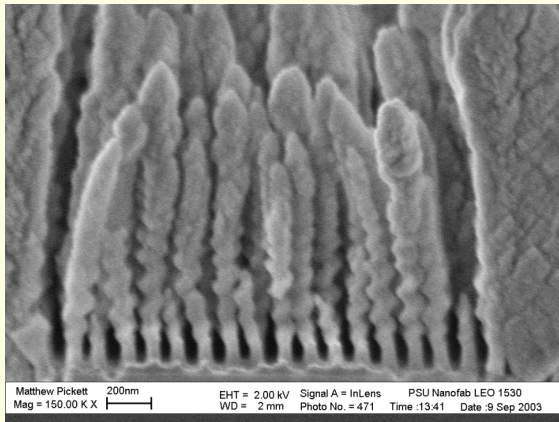


**SnO<sub>x</sub> STFs grown on photoresist patterns**

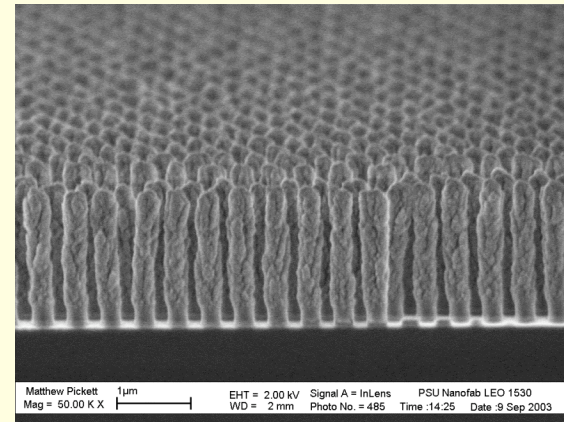
A. Lakhtakia

# STFs WITH TRANSVERSE ARCHITECTURE

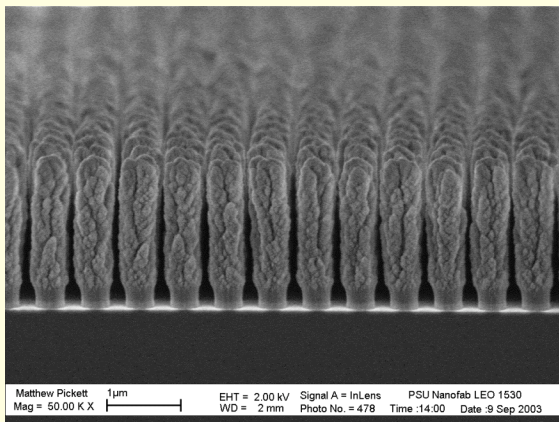
## Sculptured Nanowires on Nanoscale Topography



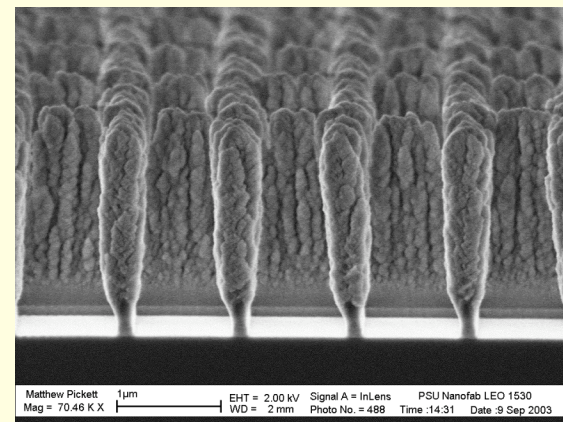
Single SiO<sub>x</sub> nanowire array grown on 60 nm e-beam resist



HCP array of SiO<sub>x</sub> nanocolumns



BCC array of SiO<sub>x</sub> nanocolumns



1µm x 1µm mesh of SiO<sub>x</sub> nanolines

A. Lakhtakia

# STFs WITH TRANSVERSE ARCHITECTURE

INSTITUTE OF PHYSICS PUBLISHING  
Nanotechnology 15 (2004) 303–310

NANOTECHNOLOGY  
PII: S0957-4484(04)69259-2

## Blending of nanoscale and microscale in uniform large-area sculptured thin-film architectures

Mark W Horn, Matthew D Pickett, Russell Messier and Akhlesh Lakhtakia<sup>1</sup>

### Selective growth of sculptured nanowires on microlithographic lattices

Mark W. Horn,<sup>a)</sup> Matthew D. Pickett, Russell Messier, and Akhlesh Lakhtakia  
*Department of Engineering Science and Mechanics, Pennsylvania State University, University Park, Pennsylvania 16802*

(Received 25 June 2004; accepted 4 October 2004; published 14 December 2004)

We have grown helicoidal nanowire assemblies on a variety of topographic substrates with regular microlithographic patterns, thereby demonstrating that sculptured thin films with transversely latticed architecture can be grown by physical vapor deposition. The transverse feature-separations are as low as 100–300 nm, and mesa regions are circular posts as small as 60 nm in diameter. The initial as well as the subsequent stages of growth on topographic substrates can be understood using simple geometric shadowing arguments. © 2004 American Vacuum Society.

# Thesis

Morphology can be nanoengineered

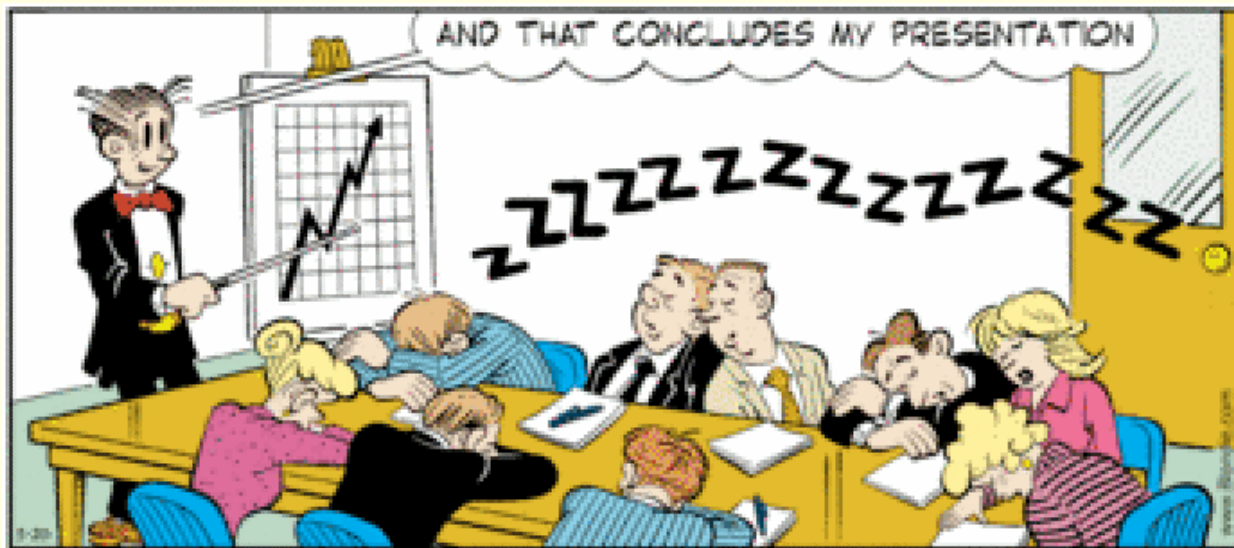
to obtain

desired polarization

&

operating frequency band

A. Lakhtakia



Thank  
You